CHAPTER – 5

PROMOTION OF MICELLAR SHAPE TRANSITION OF CATIONIC SURFACTANTS BY SELECTED INDICATOR MOLECULES

5.1. Introduction and review of previous works

Surfactant association is mainly driven by relatively weak hydrophobic and electrostatic interactions. Passing the so-called critical micellar concentration, cmc, the first type of structure usually formed is spherical micelle.[1-3] When the concentration of the surfactant increases these micelles can undergo a structural transition from spherical to rod like micelles under appropriate conditions of salinity, temperature, or addition of some organic compounds.[4-14] Depending on the range of surfactant concentrations ordered aggregates like cubic, hexagonal or lamellar phases can form as well as various disordered phases at lower concentrations can be formed. Cylindrical (Rod) micelles obtained from a mixture of surfactant and suitable salt have recently attracted considerable interest because of their unique viscoelastic properties.[15–23]

$$P = \frac{V}{L}.\frac{1}{A_0} \qquad (1)$$

The type of assembly at a certain concentration will depend on the intrinsic surfactant geometry which is well represented by the packing parameter P (Equation 1) where V and L are respectively the volume and length of the hydrophobic tail, and A_0 is the optimal surface area of the polar head group, which corresponds to the surface per molecule at which the surface free energy is minimized. Therefore, the respective requirements of the hydrophilic head group on the side of the water interface and those of the hydrophobic tails on the other side of the interface determine an optimal curvature, also called the spontaneous curvature.[24]

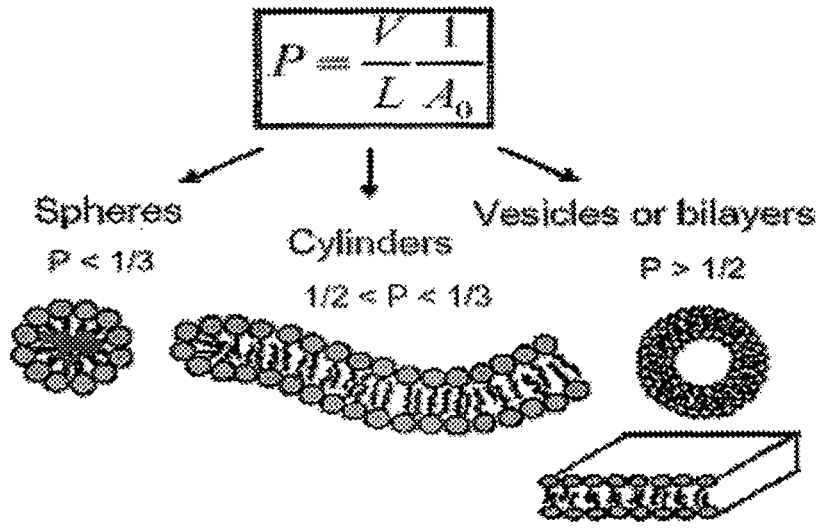

Fig. 1 Different types of micellar aggregates in relation with the geometry of the surfactant molecule

The morphology sequence and phase behaviour of surfactant aggregates is driven by the spontaneous curvature of the hydrophobic/hydrophilic interface, which does not only depend on the space filling dimensions of the surfactant molecule but may be tuned by various external factors, such as the amount and nature of added electrolyte, the presence of other species in solution, the pH or the temperature.[25] For example, if the head groups are charged, they repel each other, which increase the effective head group area and favor the formation of small spherical micelle. The addition of electrolyte tends to screen the electrolytic interactions, even more efficiently in the case of a strongly binding salt, which allow the head groups to approach each other closer and can lead to the formation of cylindrical structures. Surfactant systems show an impressive polymorphism of structures in aqueous solutions, which, in turn, influence a large variety of physical properties, in particular rheological properties.[26] Certain cationic surfactants form polymer like micelles in solutions and thus exhibit very interesting rheological properties. At high

concentrations, these solutions show typical viscoelastic behaviour. At very low concentrations, however, they show more complex and unusual rheological phenomena. Rehage and Hoffmann[27] first reported that the viscosity of a 0.9 mM cetylpyridinium salicylate solution slowly increases with time (rheopexy) when subjected to shear flow with a sufficiently higher shear rate, and that it takes an unexpectedly long time, several minutes, for the system to reach steady state. In a detailed study of the tetradecyltrimethylammonium salicylate system, they also reported that an increase in flow birefringence accompanies the stress growth. Actually both the stress and flow birefringence curves show an induction period before rapid growth commences. In addition to the general features reported before, it has been established that the induction time is inversely proportional to the applied shear rate and is independent of the flow direction. On the basis of this information, a kinetic coagulation mechanism, first proposed by Rehage, Wunderlich and Hoffmann[4] were favoured to account for the rheopectic phenomenon. According to this model, the initial small micelles collide with each other more frequently in shear flow than in quiescene, resulting in formation of large micelles. The same results are also obtained when the influence of sodium salicylate and sodium bromide concentration on the shear thickening behaviour of aqueous micellar solutions of cetyltrimethylammonium bromide (CTAB) and sodium salicylate (NaSal) is studied experimentally. The realization that there could be micelles and aggregates of different types are recent, though manifestations of unusual properties of such systems have been known for sometimes. The classic example of such an 'abnormal' system is a solution containing cationic surfactant cetylpyridinium chloride (CPC) with sodium salicylate (NaSal) as the additive.[28] These systems show strong viscoelastic effects even at extremely low volume fractions – a few millimolar concentrations.

Notable features are the observation of high viscosity even at extremely low concentrations and the existence of two peaks in the viscosity. The electron microscopic pictures of these highly viscoelastic solutions show the existence

of entangled polymeric micelles of length of several microns.[29] Two important developments, which gave clue to at least partial undergoing of these features, are:

i) NaSal is surface active and belong to the class of anionic hydrotropes.

ii) Observation of the formation of two vesicle phases (low viscosity) by Kaler and co-workers in mixed cationic and anionic surfactant systems, one phase containing positively charged vesicles and the other negatively charged.

Through this development, it becomes clear that by mixing surfactants (hydrotropes) of opposite charges, cationic and anionic, but with varying chain lengths one can control the degree of precipitation of the surfactants to produce different supramolecular structures like vesicles and polymeric micelles.[30]

It is known that certain surfactant molecules can, under correct conditions, self assemble reversibly to form large one or two dimensional (2D) structures in solutions. The one-dimensional aggregates are polymer like or rod-like micelles (depending on stiffness) whilst the 2D case represents bilayers.[31-32] In either case the structures formed can be extremely large; in the case of polymeric aggregates linear dimensions of several thousand angstroms can be obtained.[33] Experimental work on these self-assembling systems has shown that the structures have a highly non-linear response in imposed flow fields, which is a consequence of the large size and transient character of the aggregates. Rod-like micelles e.g., TTAS (tetradecyltrimethylammonium salicylate) are known to be extremely stiff in the absence of added salt one can expect the micelles to be semiflexible although it remains a sensible starting point to treat the rods as completely stiff.[34]

Single-tailed surfactants usually form globular micelles in aqueous solution above their cmc's.[35]An increase in surfactant concentration may induce the formation of wormlike micelles.[36]Similarly, addition of organic or

inorganic counterions,[36,37] uncharged compounds such as aromatic hydrocarbons,[38] or an oppositely charged surfactant[39]can transform spherical micelles into wormlike micelles. Alkyl trimethylammonium and alkyl-pyridinium surfactants are the most extensively studied surfactant systems in this respect.[40,41] Halide counterions bind moderately strongly to cationic surfactant aggregates, and therefore, micellar growth is gradual. Upon changing of the counterions to aromatic ones which usually display higher counterion binding, micellar growth already occurs at low surfactant and counterion concentrations.[42] However, not only high counterion binding is a prerequisite for micellar growth, but also the orientation of substituents on the aromatic ring is important. ^{1}H nmr studies reveal that $+N(CH_3)_3$ proton signals are shifted to higher fields and that they are broadened upon addition of salicylate counterions.[43] It was shown that the aromatic ring of salicylate is located between the headgroups and that the OH and COO^- substituents protrude out of the micellar surface.[43]Theoretical studies showed that wormlike micelles are long and flexible and that they undergo transformations on relatively short time scales.[44] This was confirmed by negative staining[45] and cryo electron microscopy,[46] which showed that wormlike micelles can become several hundreds of nanometers in length. Upon increase of the surfactant concentration, an entangled network of worm-like micelles is formed which displays viscoelastic behaviour. [35] As has already been mentioned, the rheological behaviour observed for these surfactant systems is similar to that of solutions of flexible polymers, and therefore, aqueous solutions of entangled wormlike micelles are often called living polymer systems.[40,47] Upon increase of the size of the hydrophobic portion of the counterion, the formation of vesicles has been observed. Lin *et al.*[48] studied the aggregation behavior of mixtures of hexadecyltrimethylammonium bromide (C_{16}TAB) and 5-methyl-salicylic acid. Upon changing the mole ratio of 5-methylsalicylic acid to C_{16}TAB from 0.1 to 1.1, a gradual change from spherical micelles to vesicles via wormlike and entangled wormlike micellar phases was observed. Also

sodium 3-hydroxynaphthalene-2-carboxylate (NaHNC) is able to induce the formation of vesicles in aqueous solutions of C_{16}TAB.[49] This system is compared to cationic surfactants since the phase behavior shows similarities to that of mixtures of cationic and anionic surfactants. The same system without excess of salt (C_{16}TAHNC) has also been studied. The critical aggregation concentration (cac) of C_{16}TAHNC is 0.03 mM,[50] which is significantly smaller than that of C_{16}TAB (1.0 mM). Aqueous solutions of C_{16}TAHNC show interesting temperature-dependent phase behaviour. Upon increase of the temperature, the system undergoes a transition from a turbid vesicular phase to a clear viscoelastic phase containing a network of entangled wormlike micelles. Fluorescence anisotropy and nmr spectroscopy showed an increase in fluidity of the aggregate surface upon increasing the temperature.[51] The phase transition has also been studied by differential scanning calorimetry (DSC) and conductivity experiments.[52] The temperature-induced morphological change has been explained using the theory of phase transitions in a 2D Coulomb gas.[53] It was shown that increasing the temperature results in a decrease of the HNC^- counterion binding; concurrently the head group repulsions between $C_{16}TA^+$ moieties in the bilayer increase which eventually leads to a change in aggregate shape from vesicles to wormlike micelles. A vesicle to micelle transition in aqueous solutions of C_{16}TAHNC can also be induced by shear [54] or by adding C_{16}TAB or NaHNC.[55] Thus, so far, most studies have focused on mixtures of C_{16}TAB and N-methylsalicylic acid [50]or NaHNC.[51,52,56-58]

In aqueous solution, cationic surfactants self assembled into a threadlike or wormlike micelles.[59,60] Typically, when a wormlike micellar solution is heated, the micellar contour length L decays exponentially with temperature.[61,62] The reason for this is that, at higher temperatures, surfactant unimers can hop more rapidly between the cylindrical body and the hemispherical end-cap of the worm (the end-cap is energetically unfavorable over the body by a factor equal to the end-cap energy Ec).Thus, because the end-cap constraint is less severe at higher temperatures, the worms grow to a

lesser extent. The reduction in micellar length, in turn, leads to an exponential decrease in rheological properties such as the zero-shear viscosity η_0 and the relaxation time t_R.[61-62] Accordingly, an Arrhenius plot of ln η_0 versus 1/T (where T is the absolute temperature) falls on a straight line, the slope of which yields the flow activation energy Ea. Values of Ea ranging from 70 to 300 kJ/mol have been reported for various micellar solutions.[62-64]

Through this development it became clear that by mixing surfactants (hydrotropes) of opposite charges, cationic and anionic, but with varying chain lengths one can control the degree of precipitation of the surfactants to produce different supramolecular structures like vesicles and polymeric micelles.[65-80] One can also produce tubules, ribbons, etc. by controlling the solubility of surfactants.[81,82] This facilitates an easy control over the aggregate structure and hence it is possible to induce transformations from vesicles to micelles by a proper choice of additives which are cationic,[83-85] anionic[86-90] or neutral.[91-93] Although a number of early investigations were carried out on surfactant-mediated solubilization of vesicles due to its important implications in biochemistry, there are very few studies describing such vesicle–micelle transition induced by temperature.[94-95]

From the foregoing discussion it is apparent that shear thickening occurs at low surfactant-hydrotropic core, because free worm-like micelles join a transient network under shear, the microstructures have been broadly named as shear induced structure or phase (SIS or SIP). However, a wide variety of worm like micellar solutions display rheological responses virtually identically to those described here but a common element in nearly all the systems is the presence of salt anions which associates strongly with the surfactant cations. For the first time it has been observed in this work that due to unique contribution of strong hydrophobic aromatic moiety and a polar hydroxy group in the molecular structures, 1 and 2-Naphthols are efficient in promoting SIS in CTAB and CPB micelles under salt free condition. In this chapter, viscoelastic behaviour of CTAB and CPB surfactants in presence of 1- and 2- Naphthols

have been investigated. Stimuli responsive properties of these systems are examined and microstructure of SIP is proposed.

5.2. Experimental

Cetylpyridinium bromide (CPB) was purchased from Aldrich Chemical Co., USA and was used as received. Sources and purification of other materials used in the present work have been mentioned in chapter 3.2 (page 21). ^1H nmr spectra were run at room temperature in D_2O on a Brüker spectrometer (Germany) operating at 300 MHz. FTIR spectra were recorded on a Shimazu FTIR spectrophotometer (Japan, Model:08300). Solution pH was measured by a Systronics (India) pH meter (Model: 361).

For the steady state viscosity measurement, solutions with different mole ratios of CTAB/Naphthols were prepared. Since optimum viscoelasticity was shown at 1:1 mole ratio of CTAB/Naphthols, when induced measurement was done at 1:1 mole ratio but at various concentrations (e.g., 1mM, 5mM, 10mM). Both 1- and 2- Naphthols are practically insoluble in water at low pH but soluble in surfactants. Therefore, appropriate amount of 1- and 2-Naphthols were added directly to CTAB or CPB solutions. In some experiments dilute alcoholic solution of naphthols were used and alcohols were dried off before the addition of surfactant in the experimental set. Utmost care was taken to prepare Naphthol-CTAB or Naphthol-CPB solutions with minimum shaking. The samples were equilibrated at desired temperatures in a thermostat for 2 days before study. For rheological experiment, an Anton Paar digital viscometer (Model: DV - 3PR), Austria, with low viscosity adapter was used. This is a rotational viscometer with the facility of applying variable shear. Here, the viscosity measurement is based on measuring the torque of spindle rotating at a given speed in the sample solution kept in a concentric cylinder, which is maintained at a constant temperature. The diameter and length of the inner cylinder are 2.5 cm and 9 cm respectively, whereas, those of outer

cylinder are 2.8 cm and 14 cm respectively shear rate is calculated as rpm × 1.2236 s^{-1} (assuming the characteristics of the spindle).

5.3. Results and discussion

Aqueous CTAB or CPB (1 – 10 mM) and 1- or 2- Naphthol (1 – 10 mM in 5% Methanol) show viscosities similar to that of water. But as soon as the solutions are mixed together, a thick gel with high viscoelasticity is developed. The gel vibrates upon knocking the sample vials, which indicate their elastic behaviour. This well-defined rapid gelation indicates a definite microstructure in the gelation process. Fig. 2 illustrates how the 1- and 2- Naphthols concentrations influence the steady state viscosity of the solution at constant CTAB concentration. It is interesting to note that the viscosity has maximum value when CTAB/Naphthol (or CPB/Naphthol) is present at 1:1 ratio. This result is similar to that observed previously by other workers in CTAB-NaSal or CPB-NaSal systems. It may be argued that in this molar ratio of surfactants and Naphthols, micellar transition from sphere to worm-like micelles is facilitated and most probably the worm elongate most.

Previously, it was emphasized that as the NaSal molecule is incorporated in the micelles more and more thread like micelles grow. When concentration of NaSal is larger than that of CTAB, the excess of NaSal decreases the micellar life time. In other words, the micellar break up rates increases when excess NaSal is present. It should be pointed out that, in the solutions of higher concentrations at equilibrium, a similarly complex dependence of linear viscoelasticity on the NaSal/CTAB ratio has been reported. Shikata[15,16] has suggested that the most stable and rigid micelles are formed by the 1:1 NaSal/CTAB complex. An excess or deficiency of charge on the micelles will tend to shorten the micellar life time and size. It has been proposed that excess salicylate ion catalyses the scission of the micellar network junctions, to account for the decrease of stress relaxation time in semi-

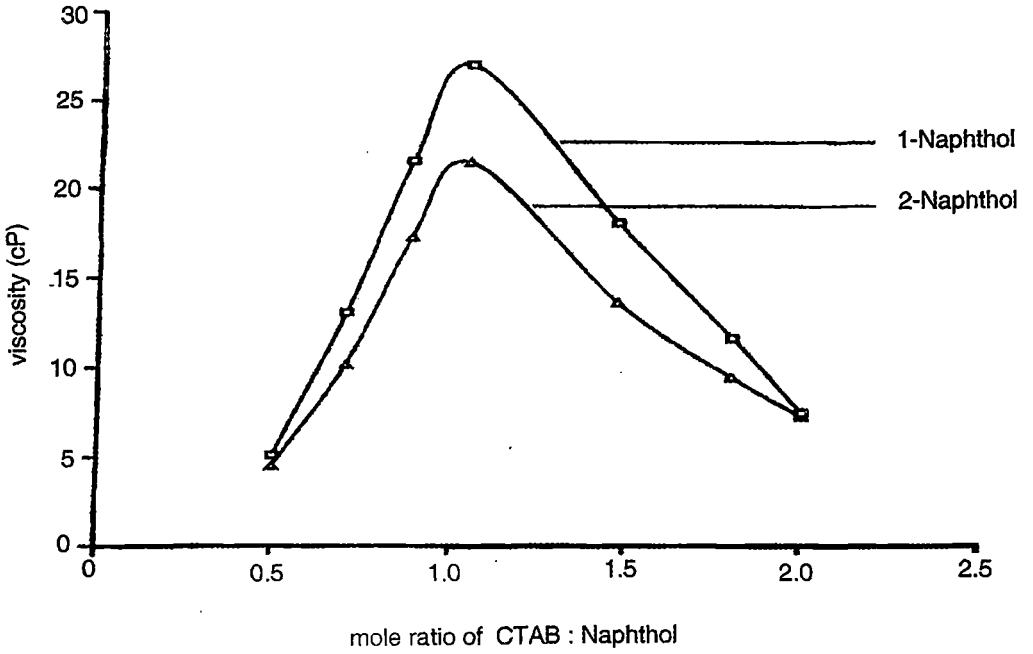

Fig. 2 Variation of viscosity as a function of mole ratio of Naphthols : CTAB.

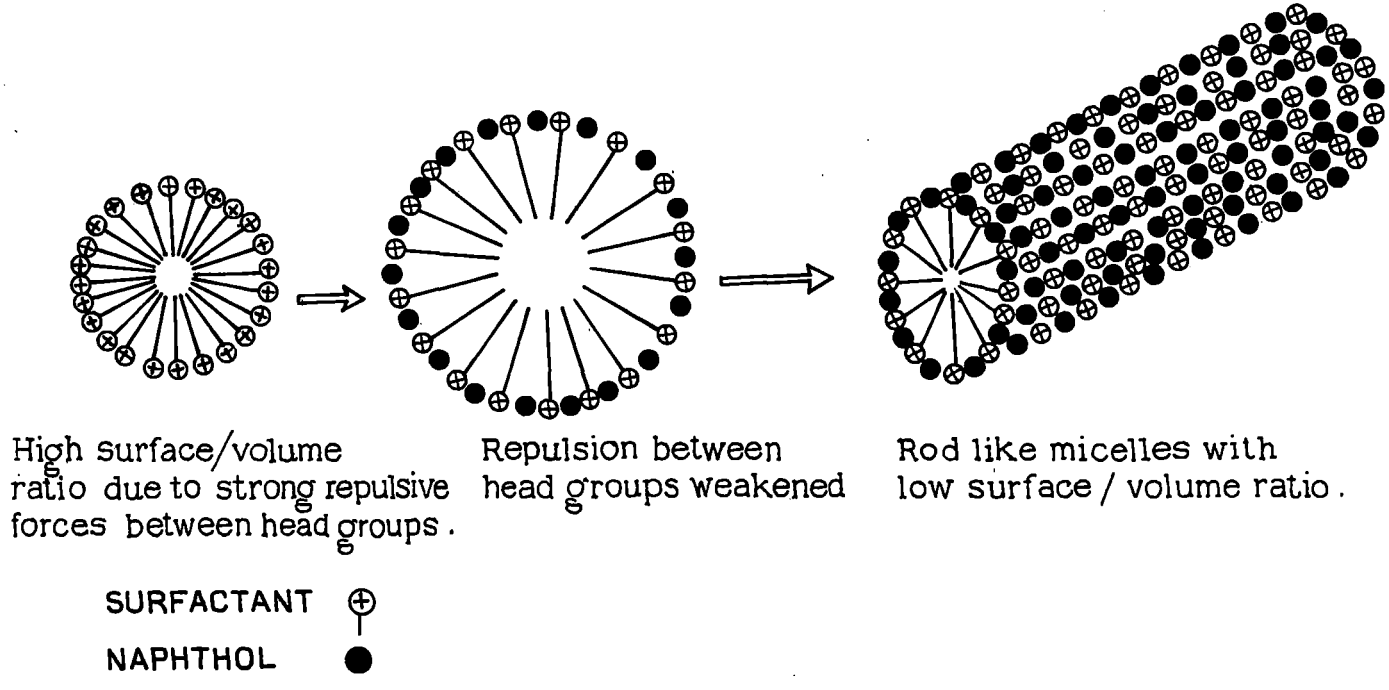

Fig. 3. Sphere to rod transition of cationic micelles in presence of naphthols

dilute solutions at equilibrium, when the NaSal/CTAB ratio becomes larger than unity. However, any explanation emphasizing the involvement of the ionic charges of the promoter molecules (viz., salicylate ion) is not apparently applicable in the present system because naphthols act in the present case as the neutral molecules. Therefore, it seems apparent that symmetrical and homogeneous distribution of surfactant and naphthol molecules (molar ratio 1:1) in the spherical micelles leading to a regular and optimal surface curvature prompted the micellar shape transition to take place (Fig. 3).

Shear induced viscosity (SIV) of aqueous CTAB-Naphthol and CPB-Naphthol systems:

At low concentrations (< 1 mM) of CTAB-Naphthol or CPB-Naphthol solutions, shear thinning features are generally observed like common non-Newtonian liquids (Figs. 4-7) upto applied shear of 200 rpm. Samples were sheared at various shear rates for a specified time with the aid of a rotational viscometer with variable shear (e.g., 10 mins) facility. This is to ensure that the high viscosity regime was reached and shear induced structure is formed.

However, at higher concentrations (1 mM-2 mM) solutions show interesting rheological properties (Figs. 8-11). Upto the applied shear rate 30 rpm, solutions shear thin. Above the shear of 30 rpm, viscosity starts increasing as a function of applied shear upto 200 rpm and SIS is formed. On further increase of applied shear, the solution viscosity decreases steadily (not shown in figure). Finite induction times are also observed before the onset of shear thickening. This is of course associated with the build up of long micellar bundles. The system recoils after the shear is withdrawn (~15 mins. figs. 12-15). Surprisingly, sheared micellar solutions take very long time, some times hours, to recoil completely and to return to an equilibrium unsheared state. Many models have been proposed, including that the microscopic structures are string like, highly aligned rods, small clusters of micelles, pearl strings of

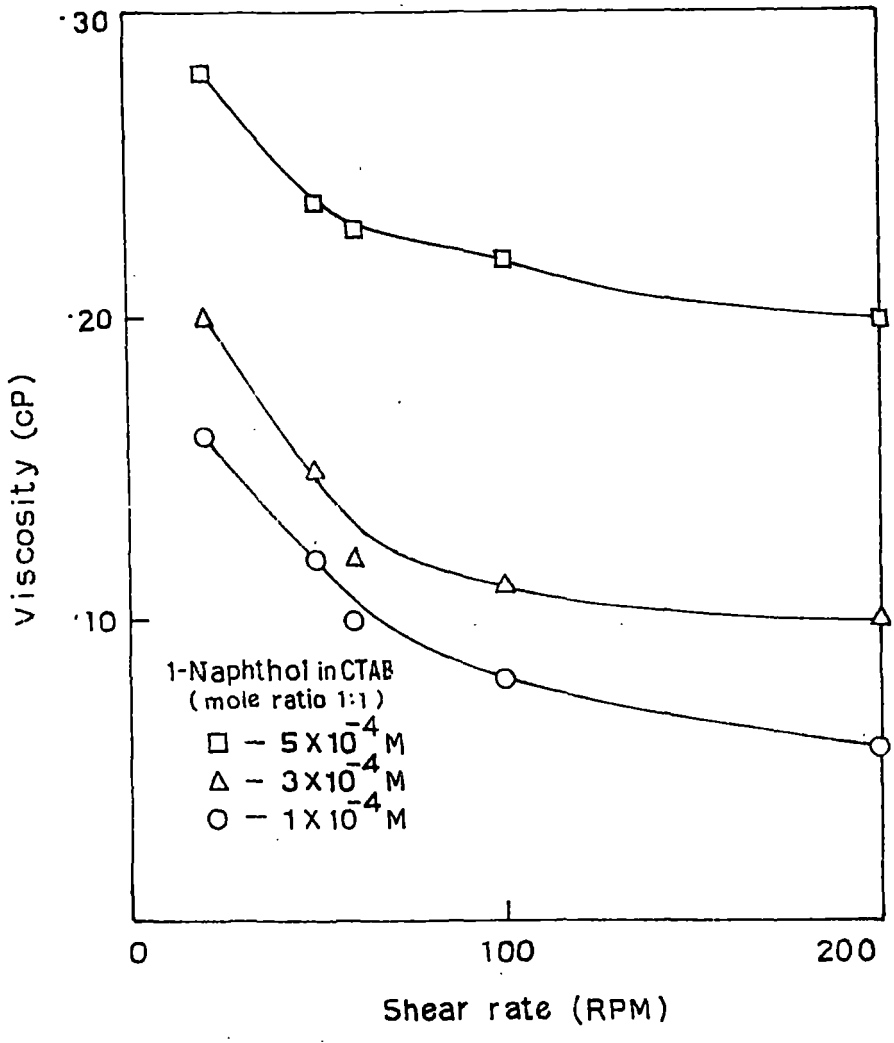

Fig. 4. Shear induced viscosity of 1-Naphthol-CTAB system at low concentration.

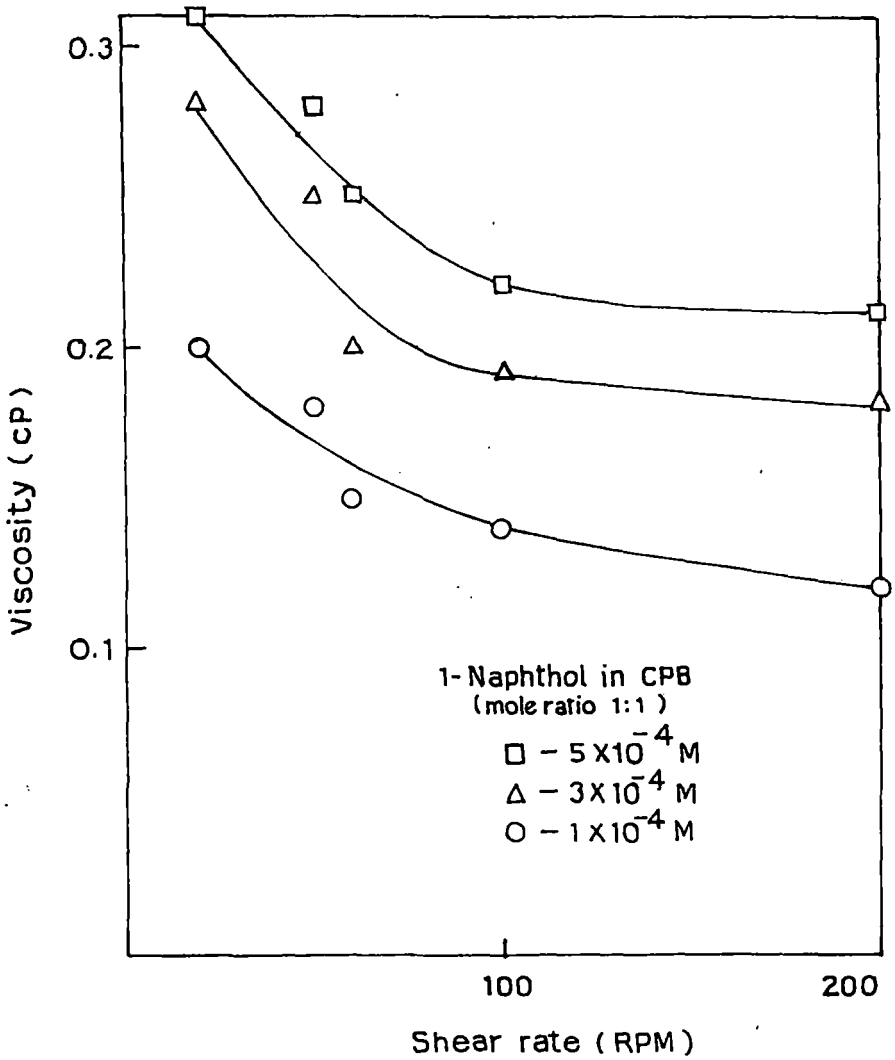

Fig. 5. Shear induced viscosity of 1-Naphthol-CPB system at low concentration.

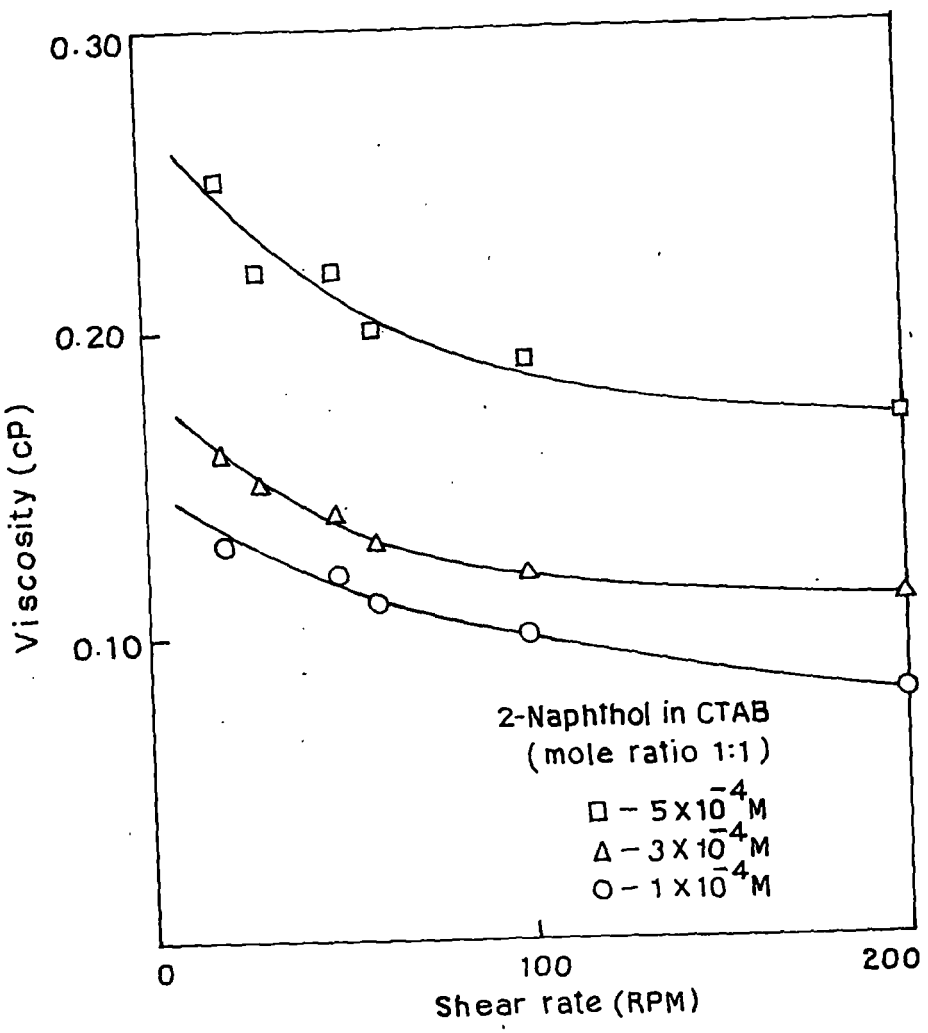

Fig. 6. Shear induced viscosity of 2-Naphthol-CTAB system at low concentration.

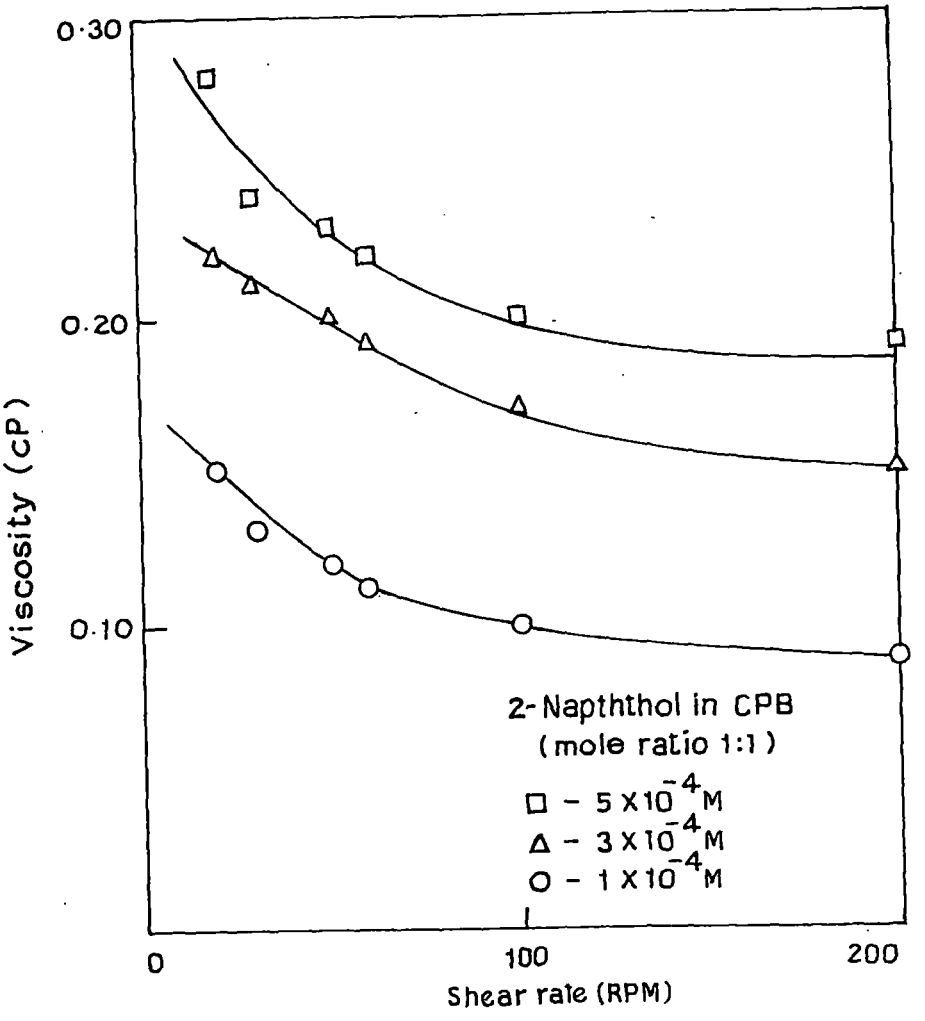

Fig. 7. Shear induced viscosity of 2-Naphthol-CPB system at low concentration.

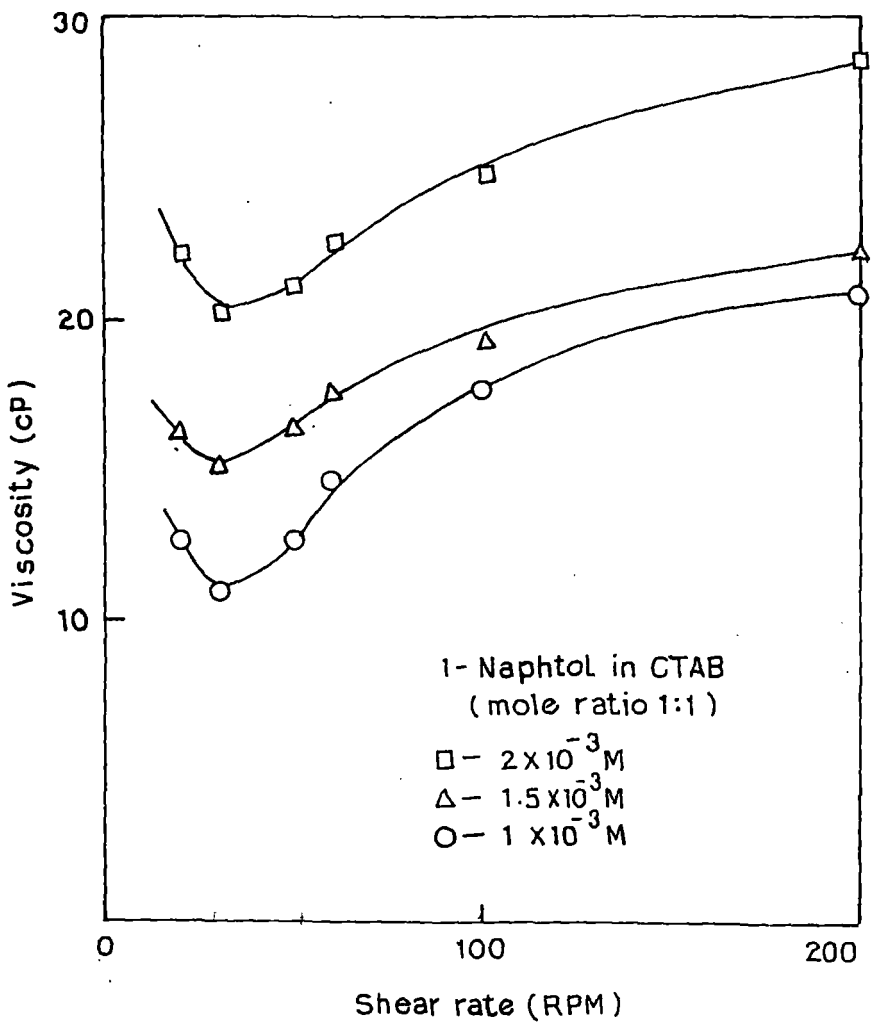

Fig. 8. Shear induced viscosity of 1-Naphthol-CTAB system at high concentration.

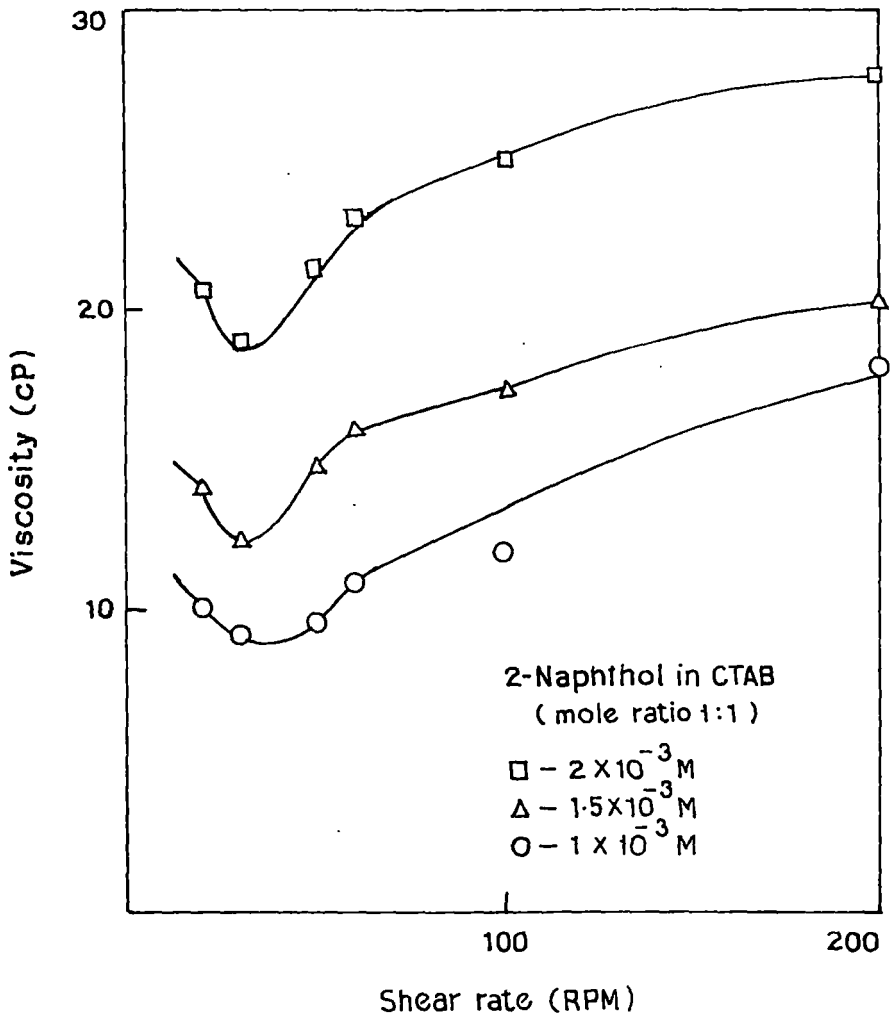

Fig. 9. Shear induced viscosity of 2-Naphthol-CTAB system at high concentration.

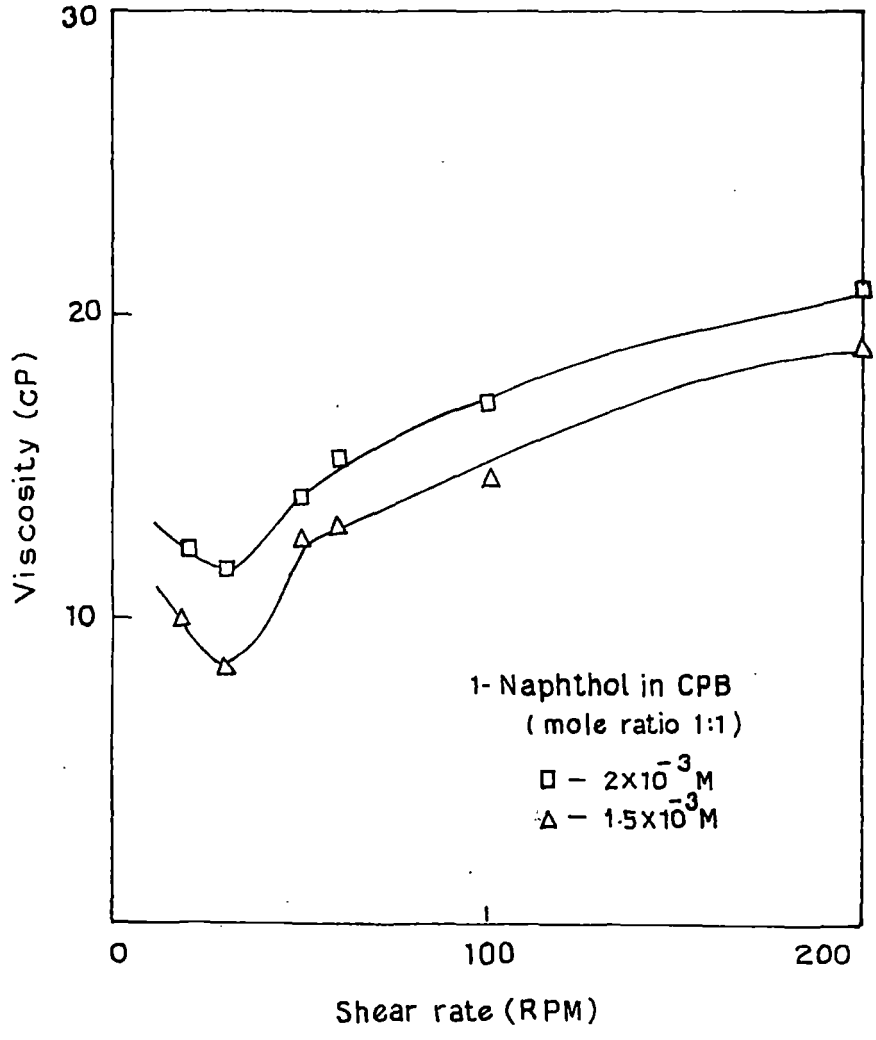

Fig. 10. Shear induced viscosity of 1-Naphthol-CPB system at high concentration.

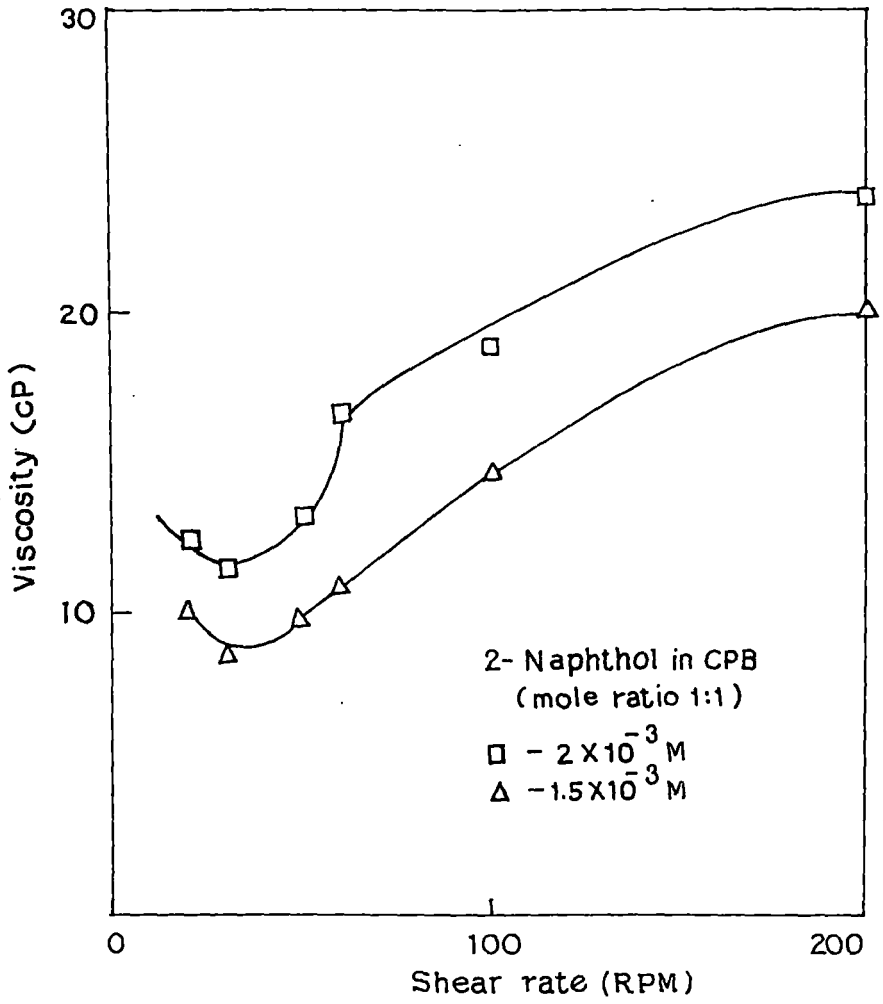

Fig. 11. Shear induced viscosity of 2-Naphthol-CPB system at high concentration.

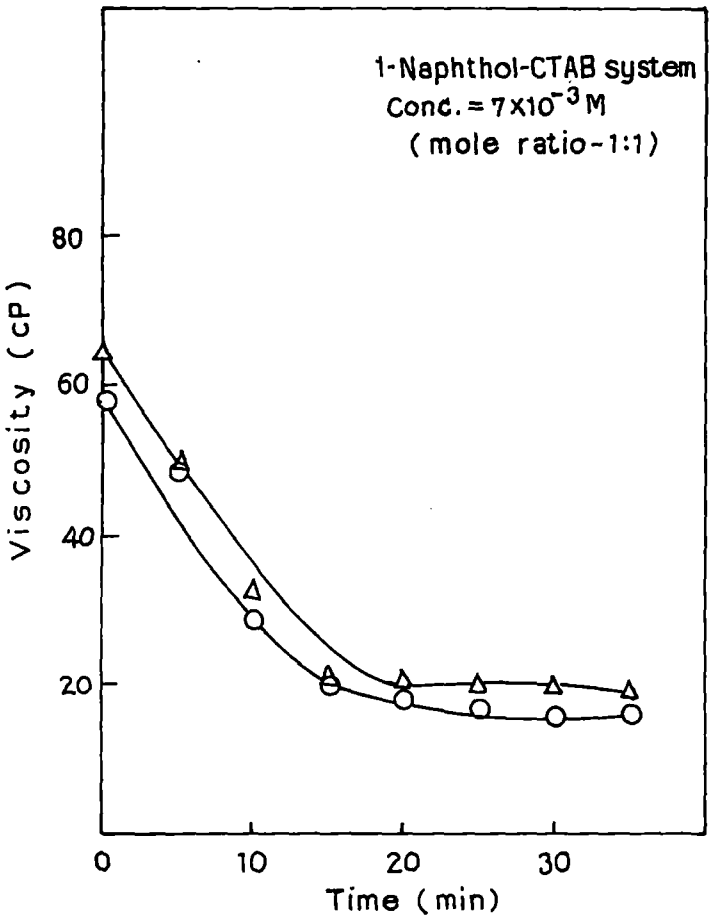

Fig. 12. Decay of shear induced viscosity with time. (applied shear = 244.72 s^{-1} at 298K), 10 mins.(○); 20 mins.(△)

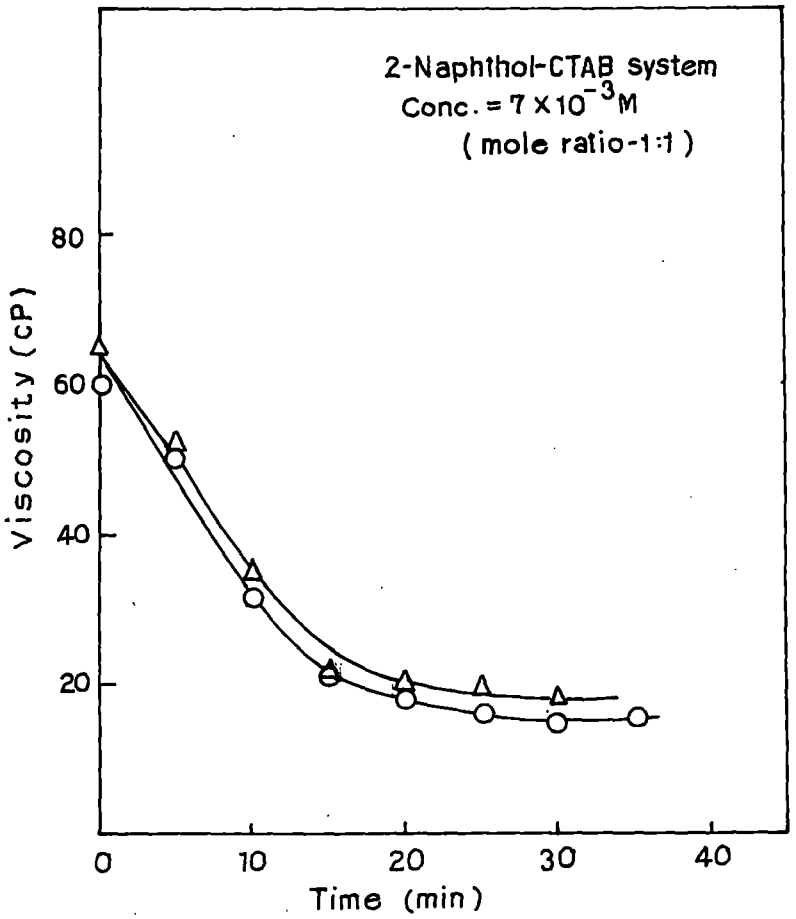

Fig. 13. Decay of shear induced viscosity with time. (applied shear = 244.72 s^{-1} at 298K), 10 mins.(○); 20 mins.(△)

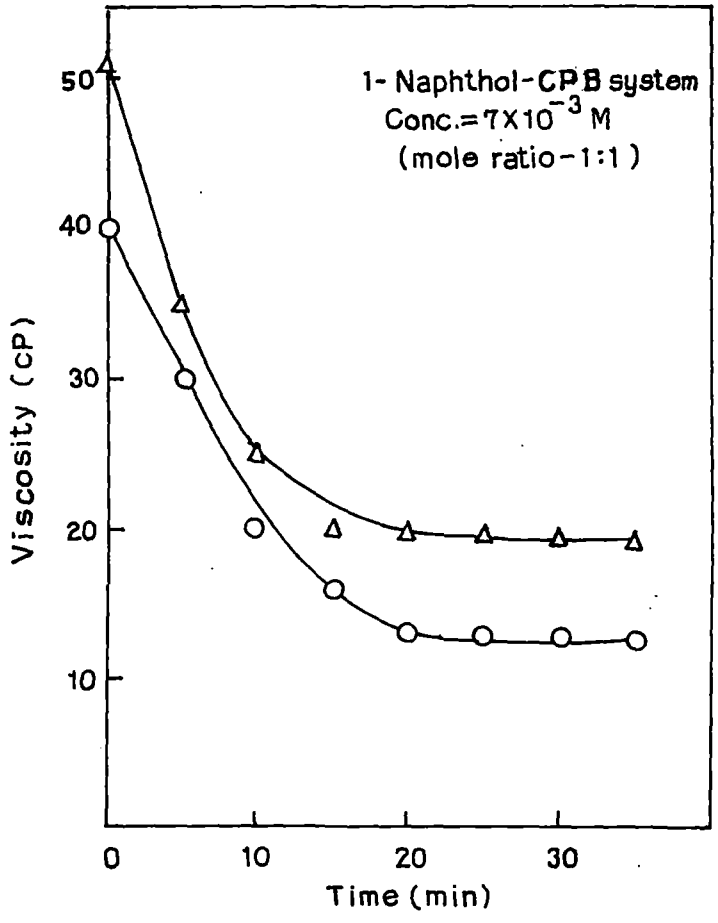

Fig. 14. Decay of shear induced viscosity with time.
(applied shear = 244.72 s^{-1} at 298K),
(O for 10 minutes,Δ for 20 minutes).

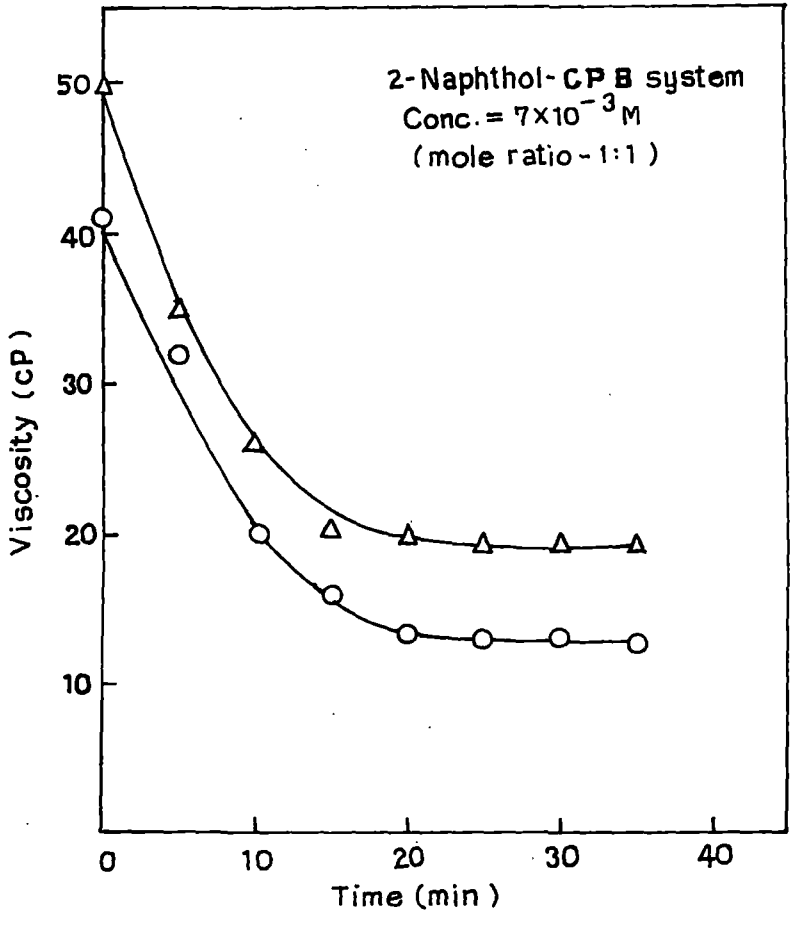

Fig. 15. Decay of shear induced viscosity with time.
(applied shear = 244.72 s^{-1} at 298K),
(O for 10 minutes,Δ for 20 minutes).

micelles, pseudonematic domains or layers of entangled wormlike micelles at high and low shear rates following reptation-reaction model.[96] The lack of direct experimental evidence to discriminate between various models has greatly impeded progress in understanding these phenomena. Previous reports on Freez-Fracture Electron Microscopy (FFEM) technique shows that the shear causes the formation of new micron sized structures that are much larger than the individual micelles and consistent with light scattering results.[96] The new structures are richer in surfactant than the surrounding micellar solution and have a sub-micron stippled or sponge-like textures. Aligned and non-aligned worm like micelles co-exist with the new structures. Also the long persistent length of the wormlike micelles suggests a high bonding rigidity. It is unlikely that electrostatic repulsion prevents worm like micelles from bending because the Debye length is only ~ 30Å in 10 mM monovalent solution. It is interesting to note that the FFEM does not show any evidence that the new structure which is developed in shear induced solution is comprised of micelles, either entangled or branched or in bundles. The bumpy structures, which are formed, resemble sponge phase of bilayers. However, the present study shows that shear induced phase is highly responsive to change in temperature (detail in next section). The gel like property disappears at slightly higher or lower temperature around the optimum one. Therefore, it is important to see that vital information regarding the SIS may not be lost due to the application of extreme temperature during FFEM experiment.

Effect of temperature and pH on viscoelasticity

Temperature dependence of viscoelasticity at different applied shear rate (fixed) are shown in Figs. 16-23 (shear rates in s^{-1} have been calculated from corresponding rpm values). Strong dependence of temperature on the shear induced viscoelasticity is apparent. Viscosity of the solution is measured at different temperatures after applying constant shear for 10 minutes. Maximum

viscoelasticity is shown at ~ 25^{0}C. However, the gel melts completely above 40^{0}C. Below 15^{0}C, also shear induced viscoelasticity disappears completely. Thus, thermoreversible property of gel indicates that shear induced on entanglement leads to SIS which is stable within the temperature of 15- 40^{0}C only in the present concentration conditions.

Effect of temperature on the viscoelastic property of CTAB-naphthol and CPB-naphthol systems is intriguing. Typically, when a wormlike micellar solutions is heated, the micellar contour length decays exponentially with temperature. At higher temperatures, surfactant unimers can hop more rapidly between the cylindrical body and the hemispherical end cap of the worm (the end cap is energetically unfavourable over the body by a factor equal to the end cap energy).Thus, because end cap constraint is less severe at higher temperatures, the worms grow to a lesser extent. The reduction in micellar length, in turn, leads to an exponential decrease in rheological properties such as the viscoelasticity and relaxation time. However, an opposite trend in the rheological behaviour is observed in CTAB-naphthol and CPB-naphthol systems as above. Instead of a decrease in viscoelasticity, it is increased with temperature steadily upto the critical temperature value and then decreases (figs. 16-23). This transition as a function of temperature is reversible, i.e., if the temperature is lowered at the critical temperature, viscosity of the system is found to decrease and approximately follow the same viscosity-temperature profile. This observation is unusual and the only example of this kind is found in a recent reference where wormlike micelle formation was promoted by excess hydroxy-naphthalenecarboxylate salt.[97] It has been argued that due to the presence of strong hydrophobic naphthalene ring in the above promoter molecules, excess salt ions become soluble in the micellar core than that of surfactant molecules causing a residual opposite charge to grow on the micelles. However, at higher temperature the observed micellar growth has been attributed to the desorption of weakly bound excess promoter ions from the micelles reducing the charge density at the micellar surface. This reduction

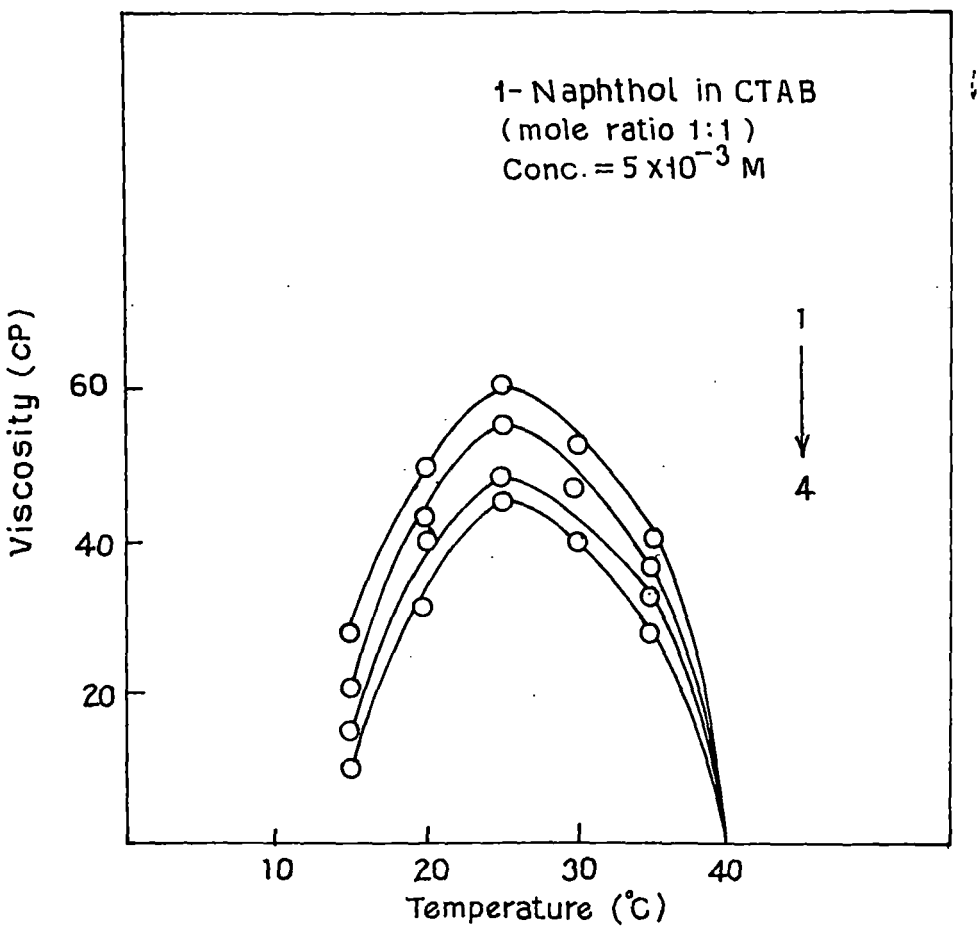

Fig. 16. Shear induced viscosity as a function of temperature. Applied shear (10 minutes): 36.71 s^{-1} (1); 73.42 s^{-1} (2); 122.36 s^{-1} (3); 244.72 s^{-1}(4).

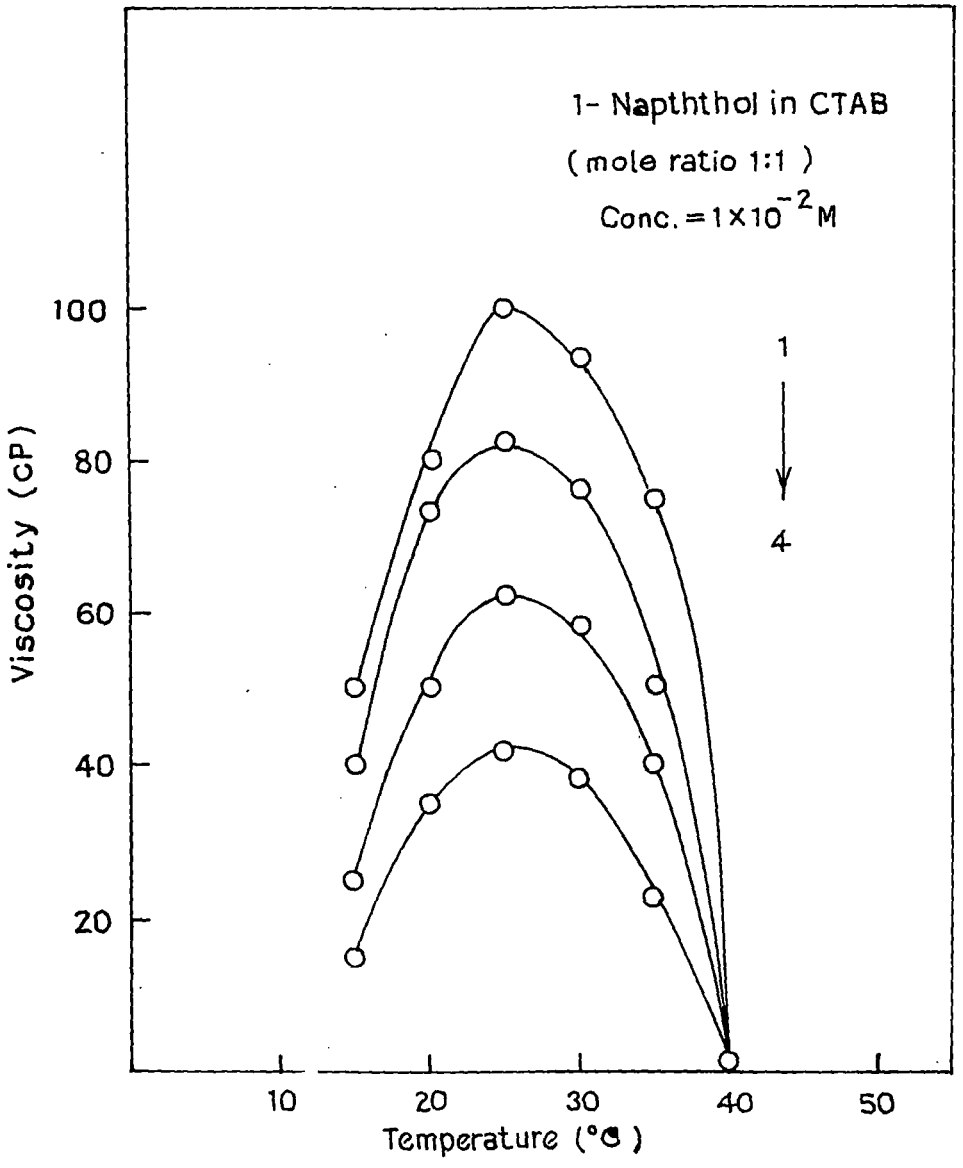

Fig. 17. Shear induced viscosity as a function of temperature. Applied shear (10 minutes): 36.71 s^{-1} (1); 73.42 s^{-1} (2); 122.36 s^{-1} (3); 244.72 s^{-1} (4).

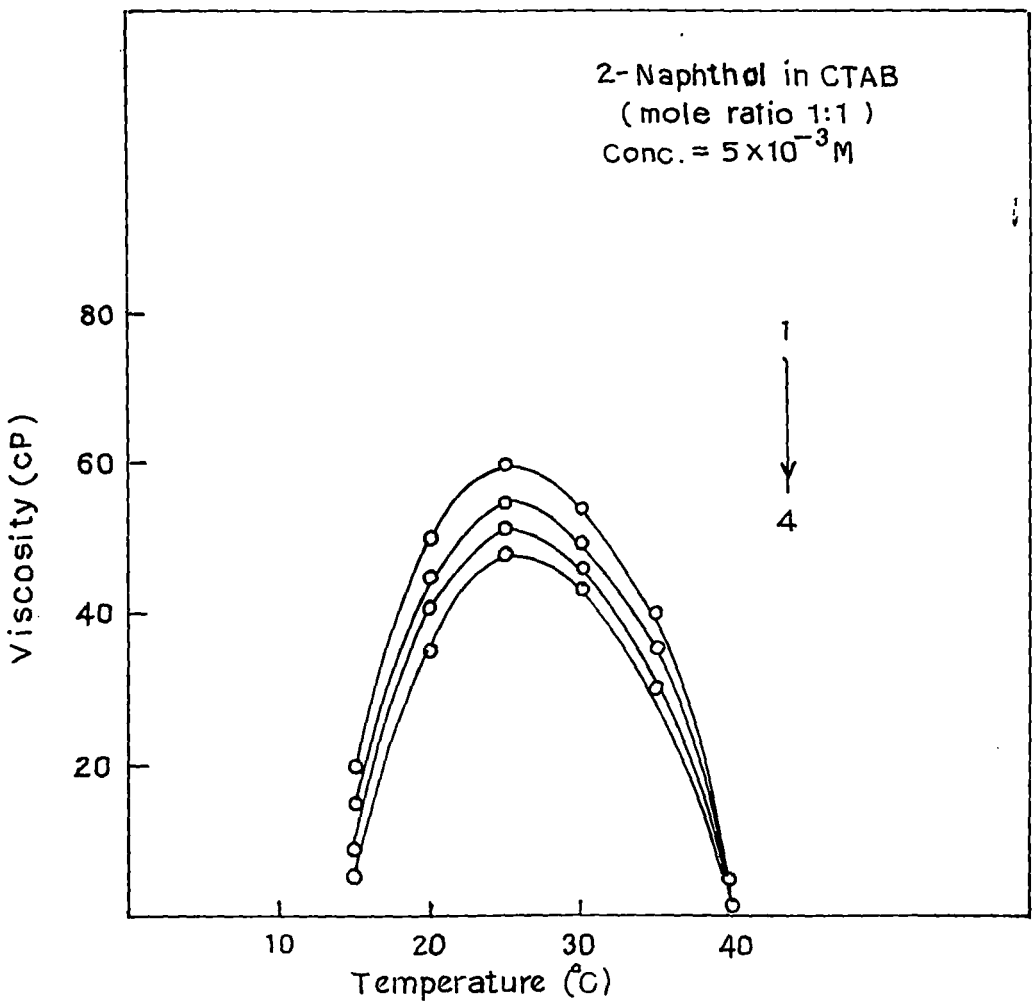

Fig.18. Shear induced viscosity as a function of temperature. Applied shear (10 minutes): 36.71 s^{-1} (1); 73.42 s^{-1} (2); 122.36 s^{-1} (3); 244.72 s^{-1}(4).

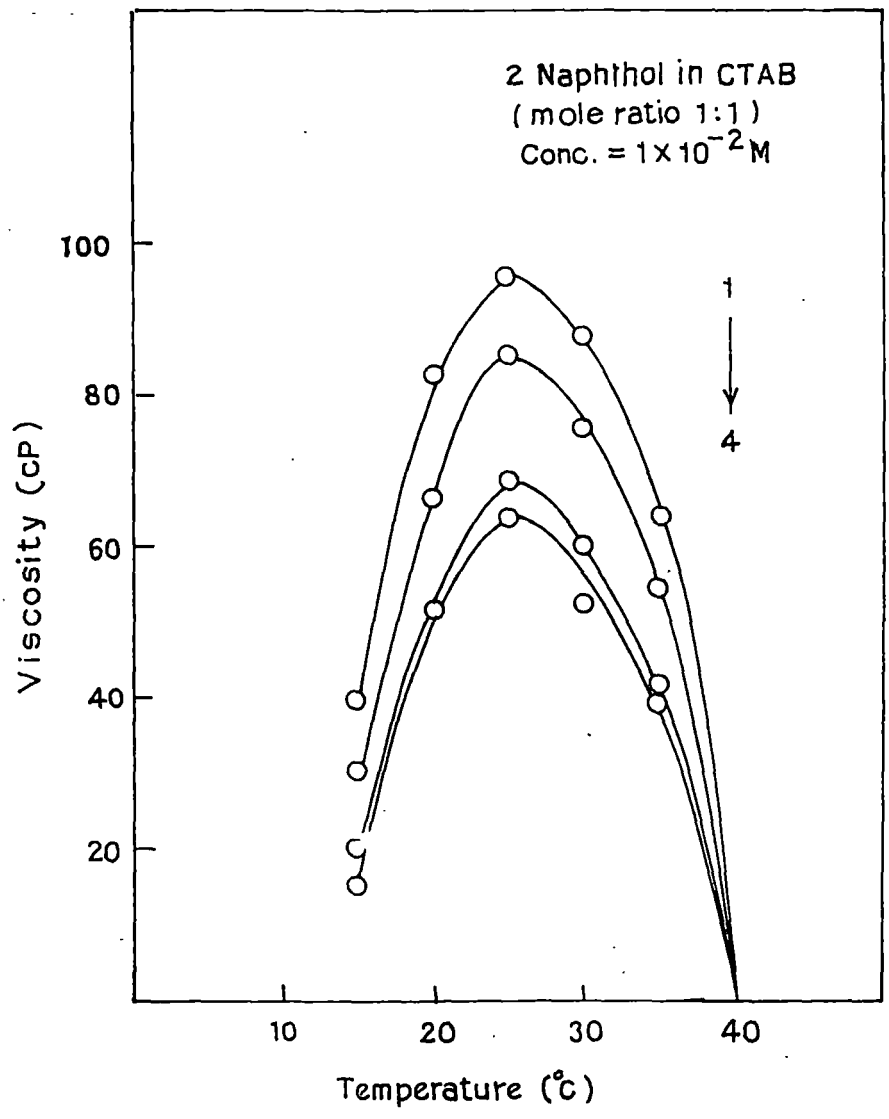

Fig. 19. Shear induced viscosity as a function of temperature. Applied shear (10 minutes): 36.71 s^{-1} (1); 73.42 s^{-1} (2); 122.36 s^{-1} (3); 244.72 s^{-1} (4).

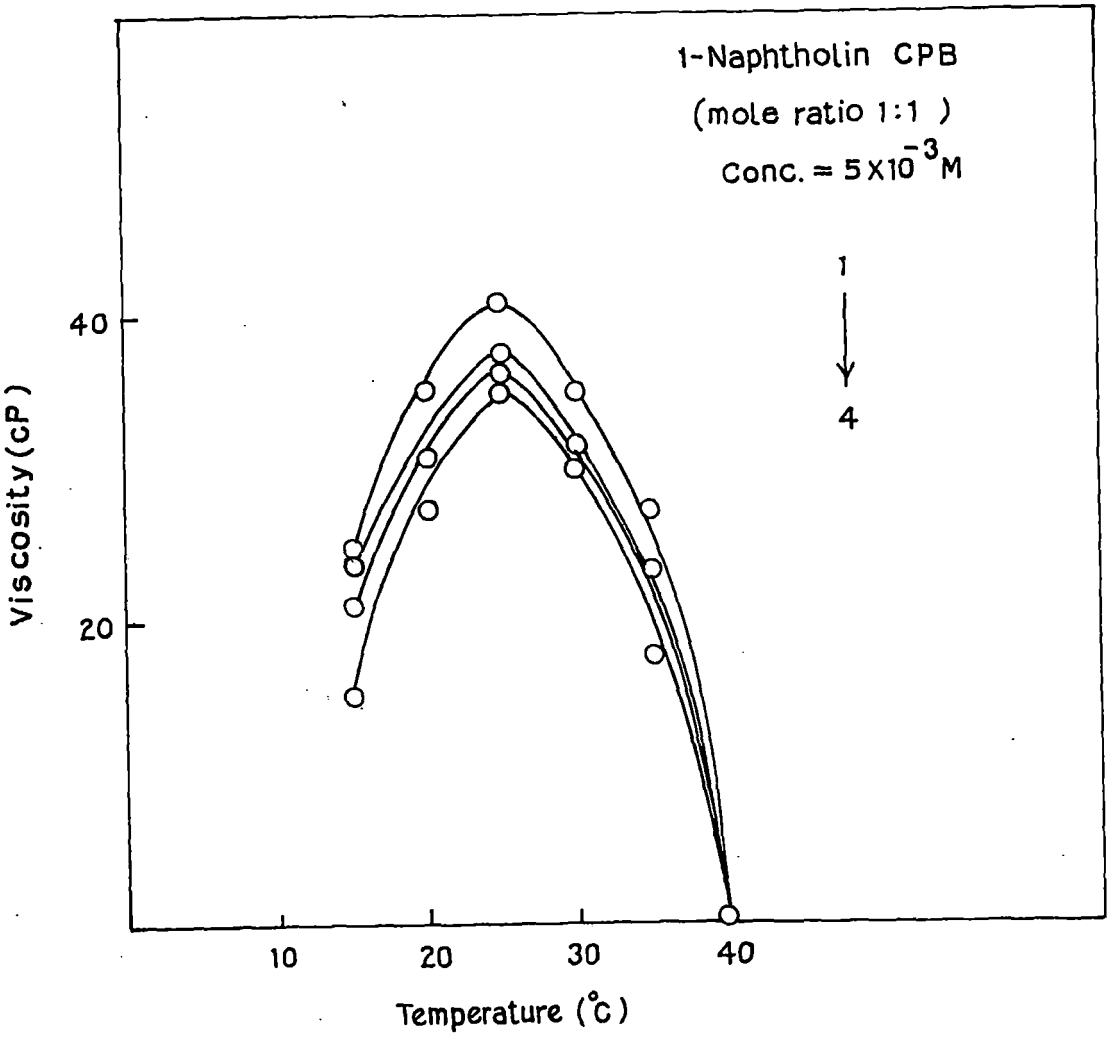

Fig. 20. Shear induced viscosity as a function of temperature. Applied shear (10 minutes): 36.71 s^{-1} (1); 73.42 s^{-1} (2); 122.36 s^{-1} (3); 244.72 s^{-1} (4).

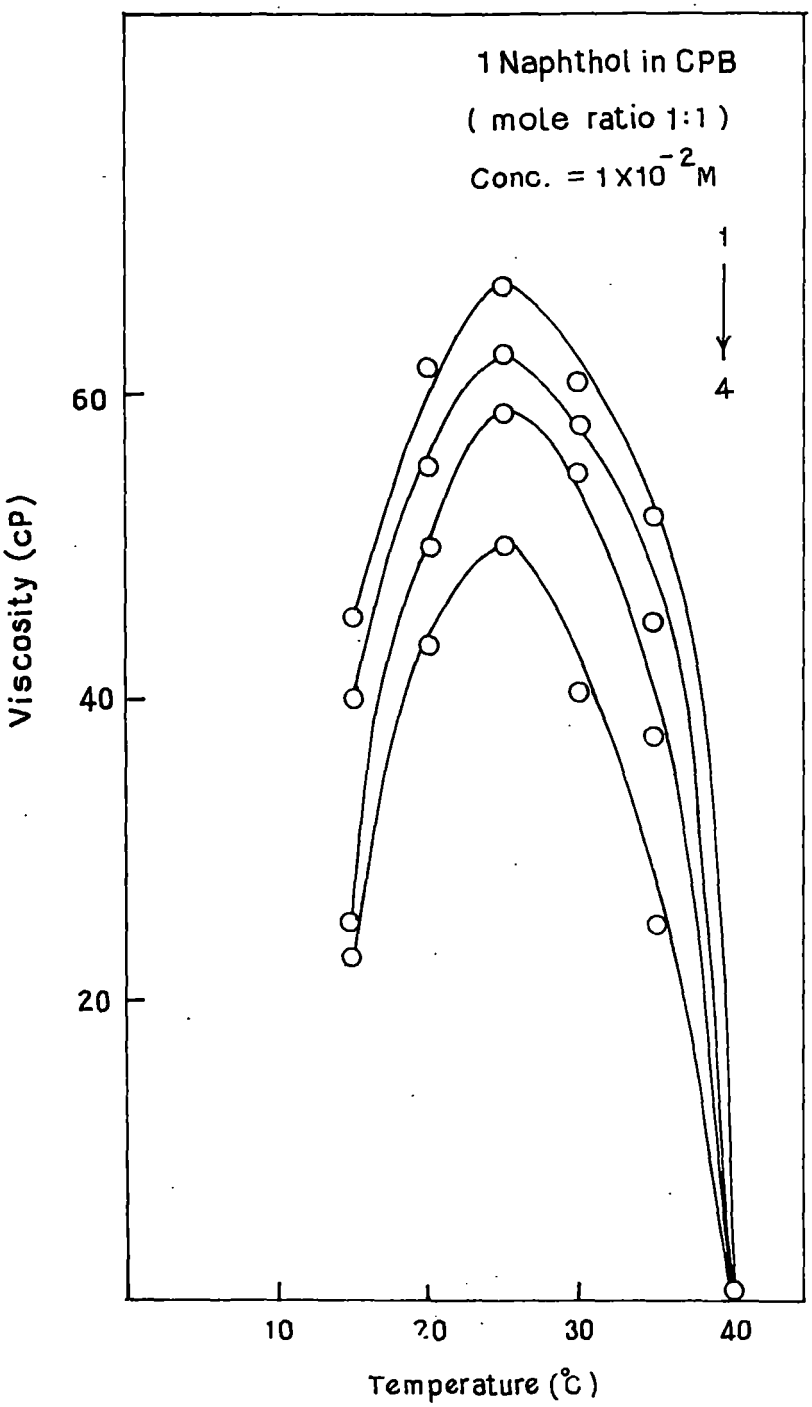

Fig. 21. Shear induced viscosity as a function of temperature. Applied shear (10 minutes): 36.71 s^{-1} (1); 73.42 s^{-1} (2); 122.36 s^{-1} (3); 244.72 s^{-1}(4).

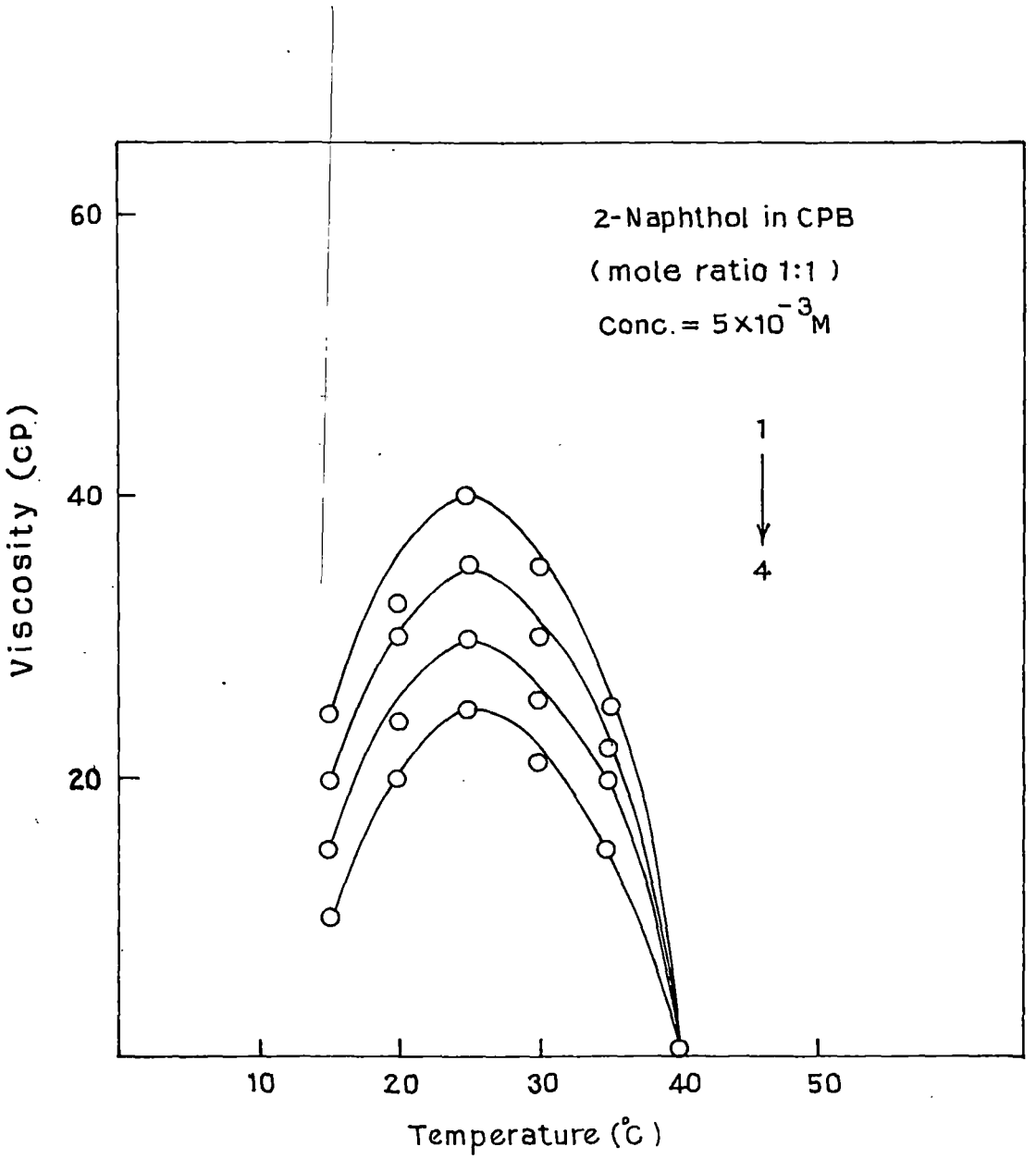

Fig.22. Shear induced viscosity as a function of temperature. Applied shear (10 minutes): 36.71 s^{-1} (1); 73.42 s^{-1} (2); 122.36 s^{-1} (3); 244.72 s^{-1}(4).

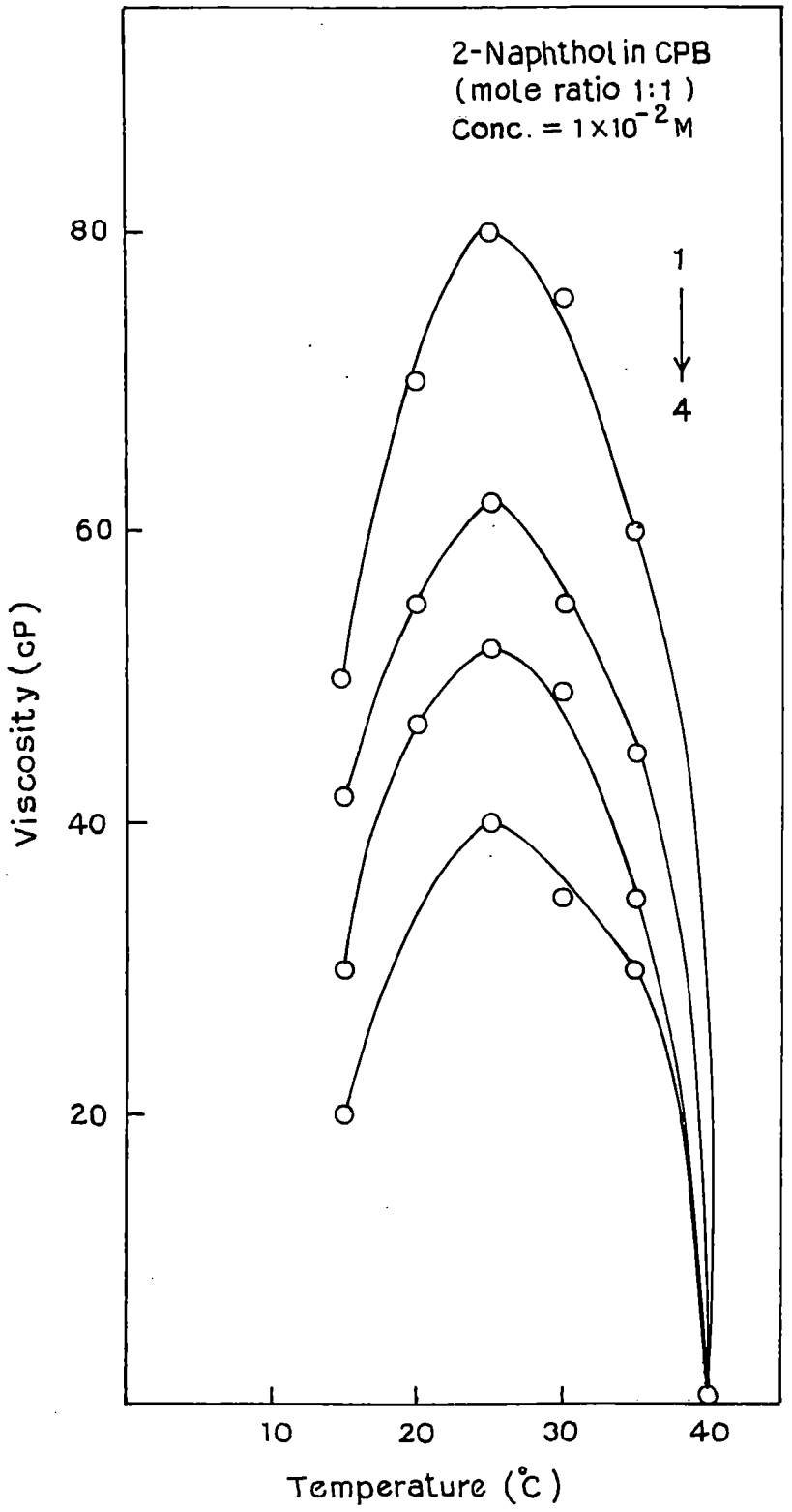

Fig. 23. Shear induced viscosity as a function of temperature. Applied shear (10 minutes): 36.71 s^{-1} (1); 73.42 s^{-1} (2); 122.36 s^{-1} (3); 244.72 s^{-1} (4).

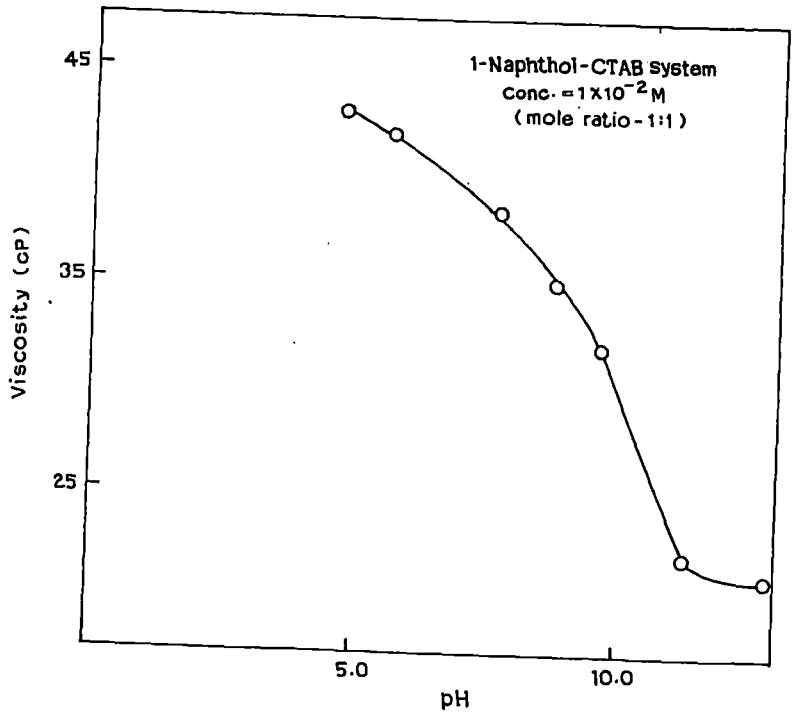

Fig. 24. Shear induced viscosity as a function of pH (applied shear = 36.71 s^{-1} for 10 minutes at 298K).

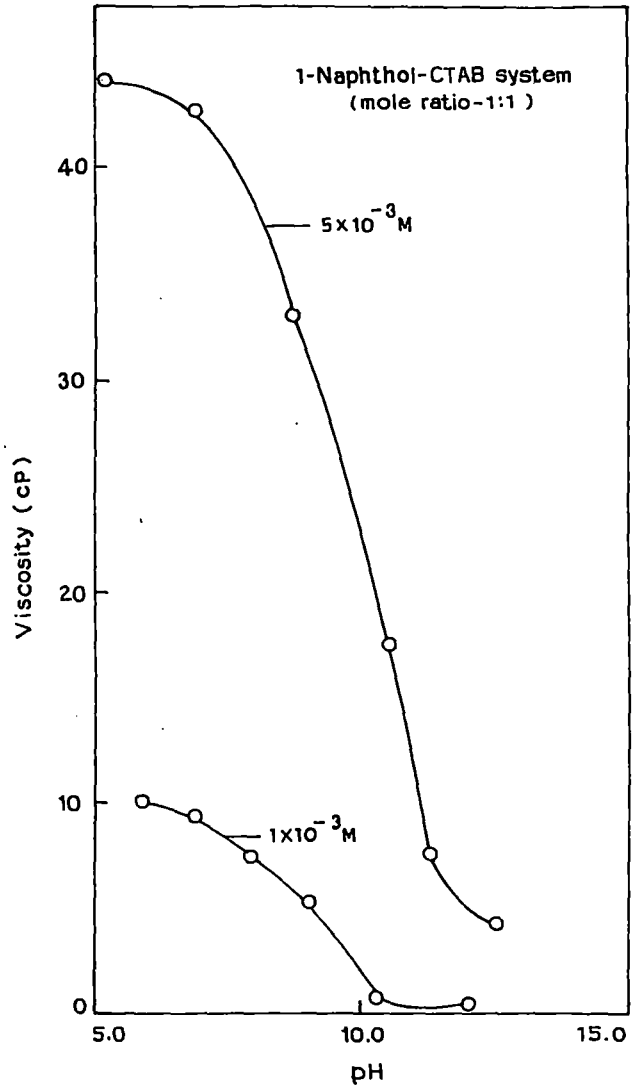

Fig.25. Shear induced viscosity as a function of pH (applied shear = 36.71 s^{-1} for 10 minutes at 298K).

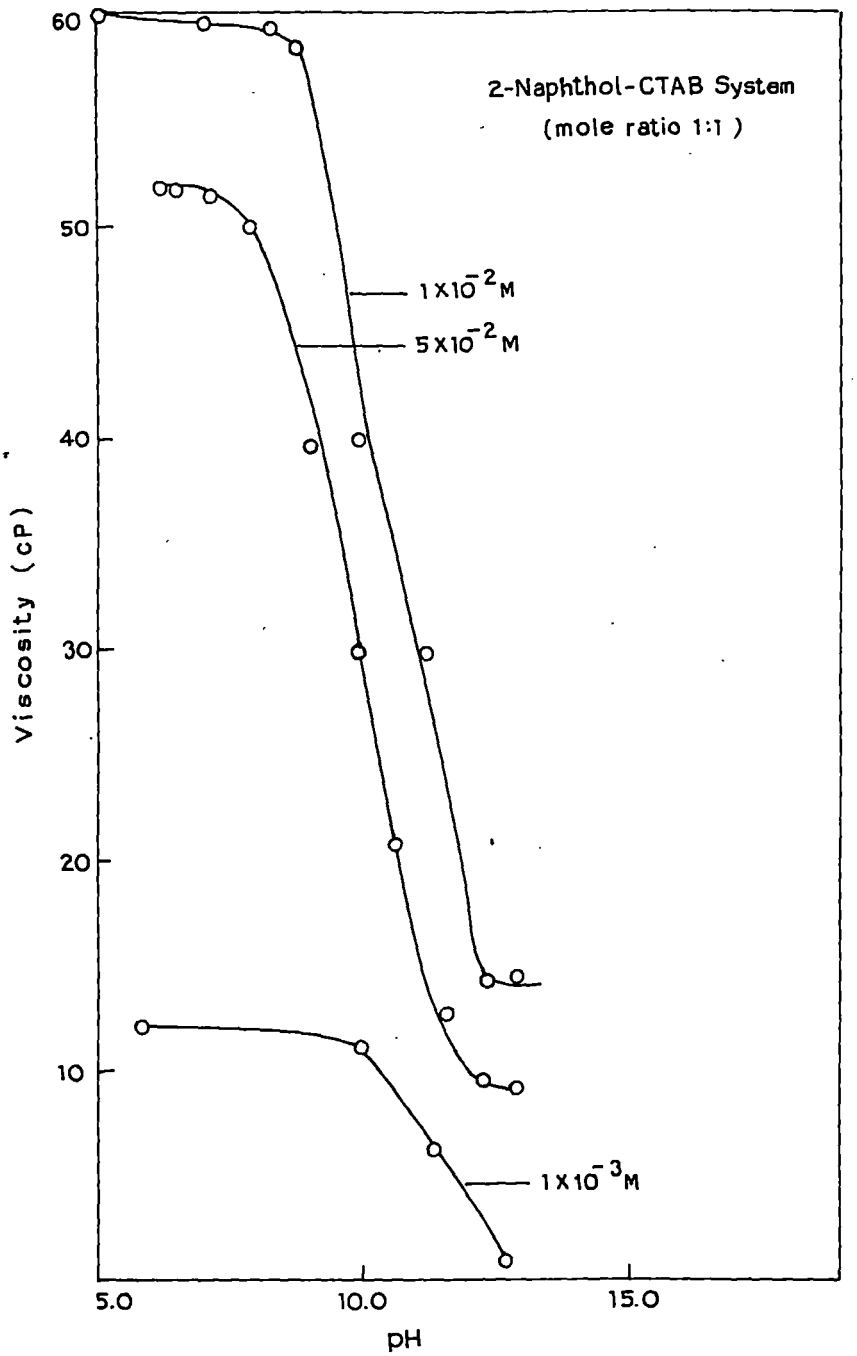

Fig. 26. Shear induced viscosity as a function of pH (applied shear = 36.71 s^{-1} for 10 minutes at 298K).

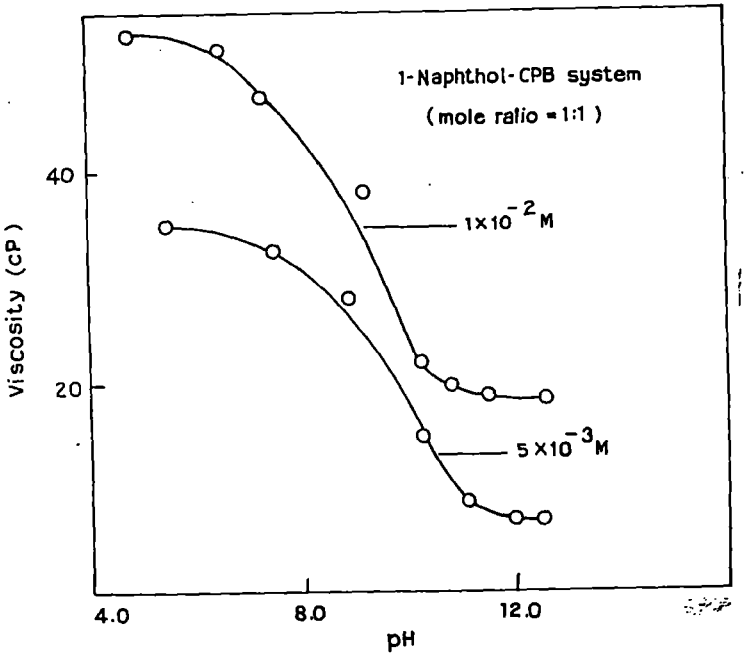

Fig. 27. Shear induced viscosity as a function of pH (applied shear = 36.71 s^{-1} for 10 minutes at 298K).

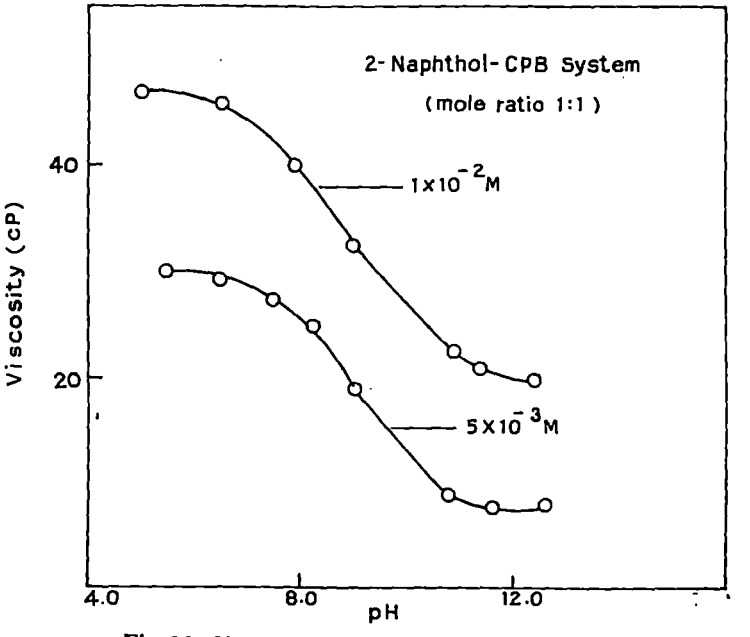

Fig. 28. Shear induced viscosity as a function of pH (applied shear = 36.71 s^{-1} for 10 minutes at 298K).

of charge density at the micellar interface promotes the growth of cylindrical micelles. However, any explanation emphasizing charge screening of micellar surface by the added salt anions as has been put forward in the above reference is again not applicable in the present system. Hydrophobic interaction between micellar core and the aromatic ring of the naphthol molecules seems to be important factor which impart thermoreversible viscoelasticity in the present systems also. But, as the temperature is increased, naphthol molecules (mostly protonated) become more and more soluble and perhaps are partitioned more strongly in the micellar hydrocarbon core. This favours the formation of longer wormlike micelle upto the critical temperature, above which the increased kinetic energy allowing surfactant unimers to hop more frequently between the body and the end cap results in the breaking up of the same.

Figs. 24-28 illustrate steady state viscosity of (1-10) mM equimolar CTAB/Naphthol and CPB/Naphthol solutions and as a function of bulk pH. Dependence of SIV on pH is also intriguing. Although SIV in most of the present systems remains virtually steady within pH range of 4.5 to 6.5 it starts decreasing thereafter. The SIV again become constant, after pH 11.0, pK_a of 1- and 2- Naphthols in aqueous medium are 9.2 ± 0.2 and 9.5 ± 0.3 respectively. When the Naphthols are bound at the aqueous micellar interface, the pK_a value will be modified slightly. It is, however, interesting to note that in 1- and 2-Naphthols, more than 50% of the hydroxyl group are ionized above pH 9.2 to 9.5 respectively, i.e., SIV decreases significantly as the hydroxyl groups are ionized. This observation is clearly indicative of the involvement of hydroxyl group of Naphthols in entanglement and/or transitional networking of micelles.

NMR and FTIR characterizations

The molecular origin of worm like micellar growth is believed to be the adsorption or insertion of the hydrotropes into the micelle and thereby altering the packing parameter of the micelles. However, screening of the charges of

head group facilitates the transition. Therefore, the location and orientation of the promoter is important factor. To determine the efficiency of the promoter molecule, the nmr spectroscopy is an ideal probe of the average position and orientation of the additives on the micellar surface. Past nmr studies of aromatic counter ions on cationic micelles showed an upfield shift in proton resonance of the aromatic moiety, from which it was inferred that the aromatic rings are inserted into the micelles.[98] In the present study, ^1H nmr spectra of pure Naphthols and CTAB and CPB in D_2O were measured. Fig.29 (inset a) shows that the spectra of 2-Naphthol in D_2O give clusters of signals centered at δ value of 7.850 and 7.382, due to the resonance of the aromatic ring proton. These two sets of signals are shifted upfield, broadened and merged to give two broad (signal) peaks at δ value of 7.337 and 6.991 respectively when 10 mM Naphthols are mixed with 10 mM CTAB in D_2O (Fig. 29; 1b). Thus large shift of aromatic proton resonance to low δ values clearly indicates the location of naphthol rings in the less polar environment than that of water. This means that the aromatic rings of the naphthols penetrates to some extent inside the non polar micellar core. On the other hand, ^1H resonance signals of Me_3N^+ head group of CTAB appears at δ value of 3.132 and the signals from $-CH_2$ group adjacent to head group appear at 3.313 and 3.289 (almost merged together)in D_2O (Fig.29; inset C). Although both of the protons signals shifted upfield, the protons of $-CH_2$ group adjacent of the tetramethyl ammonium $N(CH_3)_3$ head groups of CTAB are affected most due to the presence of naphthols (above two signals are shifted to 2.746 and 2.379 respectively, (Fig. 29; 1d). Signal from $-CH_2$ protons emerge on the other side of the $N(CH_3)_3$ peak. This identification is important because it indicates the presence of aromatic ring of the additive resides near the head groups but it is more close to the $-CH_2$ group, which are at immediate vicinity of the head group. This feature in conjunction with corresponding shifts of the aromatic protons of the solubilisate molecule conclusively proves that the solubilized molecule sits near the surface of the micelle with a well-defined orientation. The spectral feature is also suggestive

of the fact that the naphthol molecules are not penetrated deep inside the micellar core but present near the surface with hydroxy probably protruded from the micellar surface and screen the surfactant head group charges. Fig. 29; 2 shows spectra at high concentration of naphthol and CTAB. Due to stronger gel formation, the signals broadened.

Because FTIR is also a powerful tool to investigate the microstructures of gel system, we have used this technique also to investigate the structure of micellar entanglement. Fig. 30 and 31 show IR spectra of 1-Naphthol in presence and in absence of CTAB and CPB respectively. During sample preparation, naphthols and CTAB or CPB were mixed together at 1:1 mole ratio and shear was applied (200 rpm for 10 mins). The aqueous gel then dried at 25^0C temperature under vacuum for 24 hours or until the drying was found complete (since gel melts at high and low temperatures). Fig. 30 illustrates spectral feature of –OH stretching band in absence of CTAB (A) and that in presence of CTAB (B). It is observed that the gelation leads to a significant change in IR spectra. The broad band at 3354 cm^{-1} associated with –OH stretching of 2-Naphthol shifts to 3163 cm^{-1} (not sharp) upon micellar entanglement. In CPB micelles, this shift is even much prominent (shifts to 3100 cm^{-1}, Fig. 31). This large shift to lower frequency clearly indicates that even though weak intermolecular hydrogen bonding may be present in naphthols, it is still very strong when they are involved in bridging a number of long wormlike micelles leading to three dimensional network. Thus, the microstructural diversity associated with the intermolecular H-bonding in napthol, which results in the diffused and broad energy states of the excited normal modes no longer exist in gel. A comparatively more well defined and specific H-bond is present in gel, which may bridge wormlike micelles together to form the network structure. The peak at 3050 cm^{-1}, which remains almost unchanged upon gelation, may be assigned to aromatic –CH stretch. The shear induced phase is highly entangled viscous, strongly aligned, and consists of structure much larger than individual micelles. Present study undoubtedly show

that naphthols embedded in different micelles bridge between the micelles resulting in the entanglement. This is perhaps the first direct proof of involvement of hydrogen bonding in mecellar entanglement. The micron-sized structures, which are much larger than individual worm like micelles and are formed on the application of shear are also formed probably via hydrogen bond networking (Fig. 32). These percolating superstructures are responsible for the increase in viscosity, consistent with the observed shear thickening.

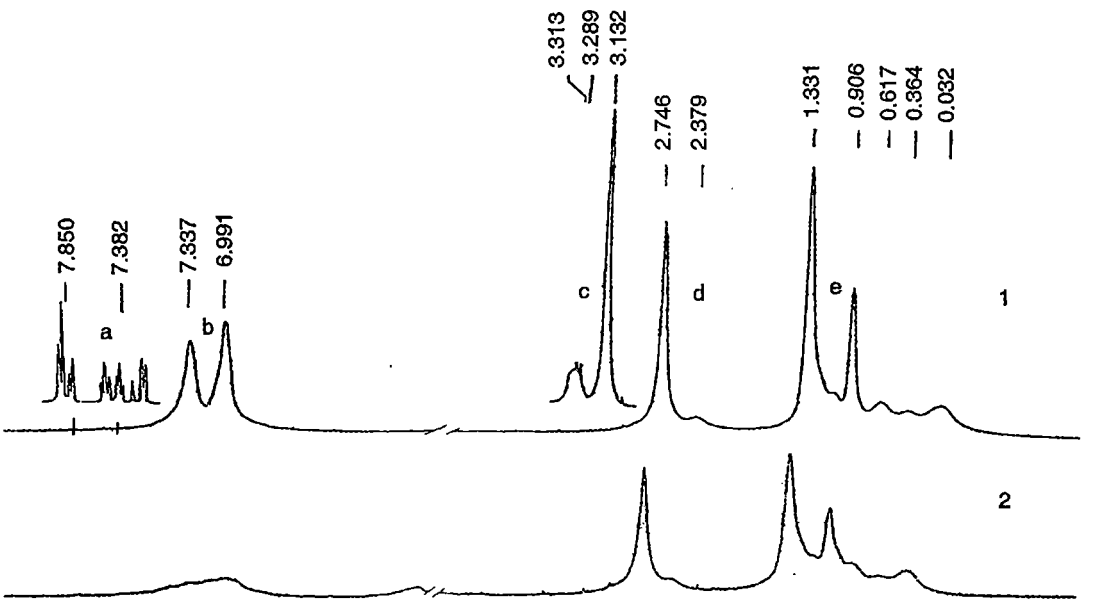

Fig. 29 ^{1}H nmr spectra of 2-Naphthol-CTAB system.

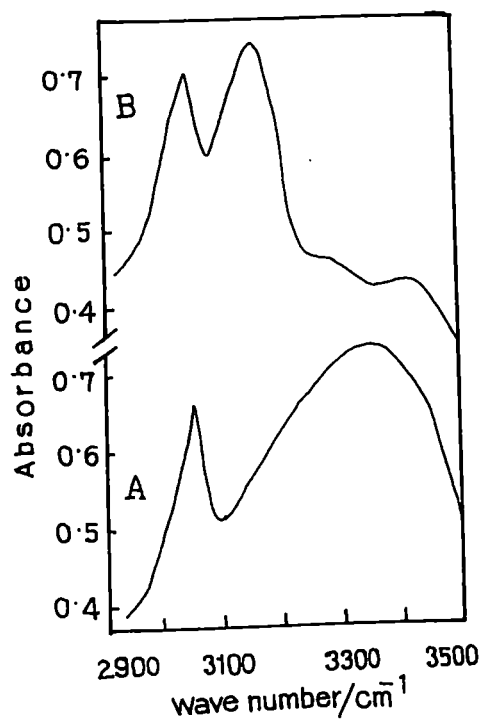

Fig. 30. FTIR spectra of 2-Naphthol in absence (A) and in presence of CTAB micelles (B).

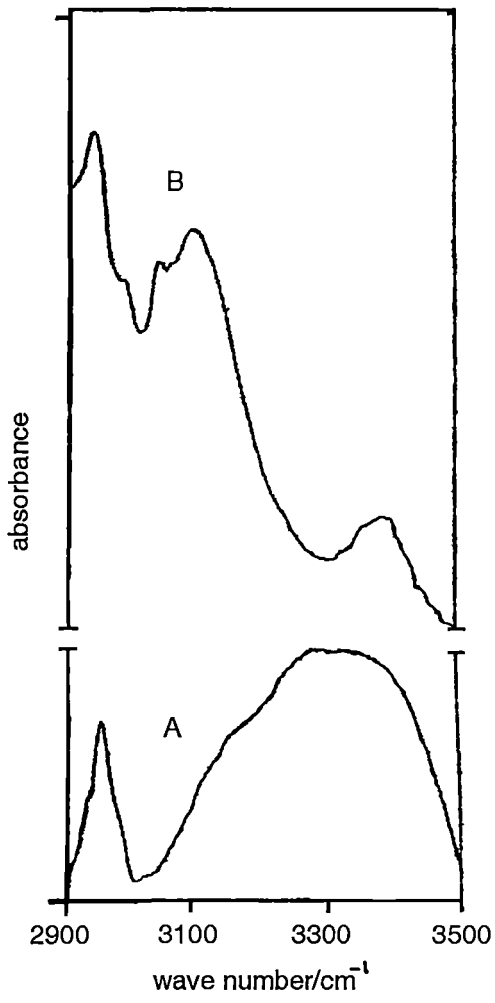

Fig. 31. FTIR spectra of 2-Naphthol in absence (A) and in presence of CPB micelles (B).

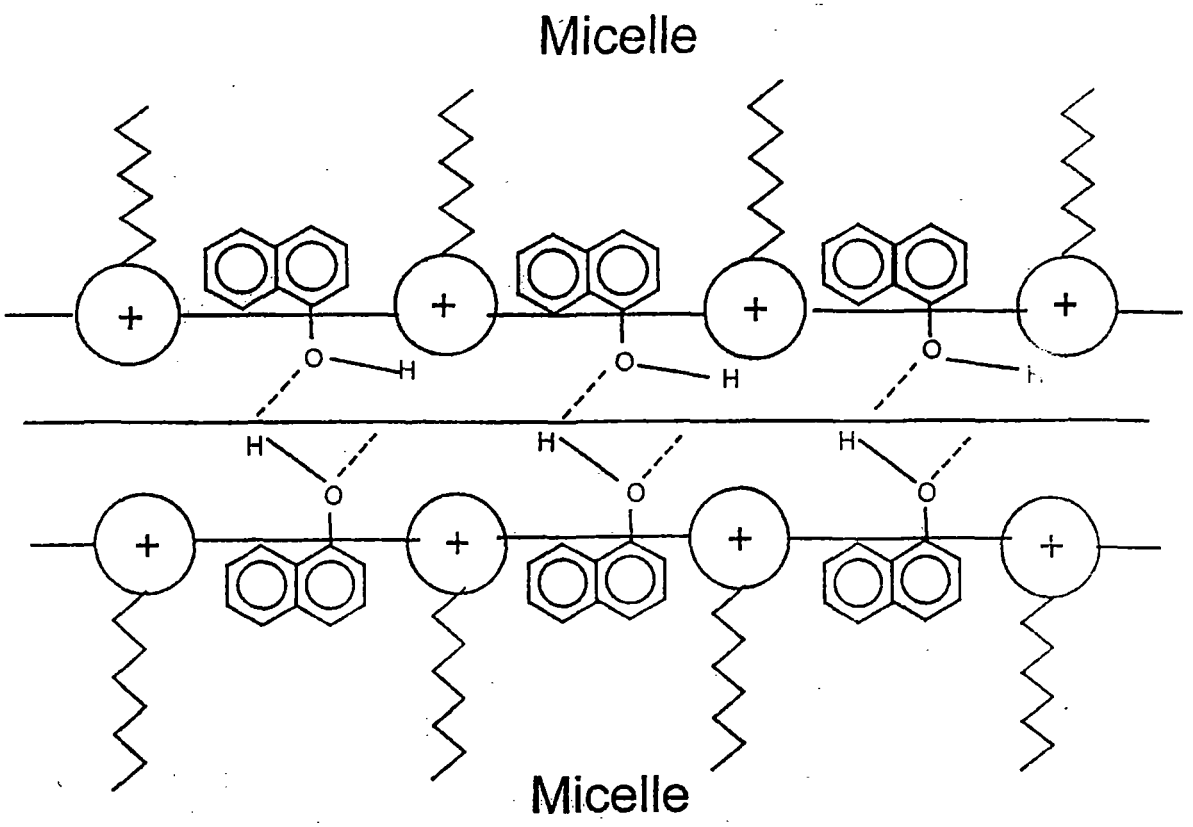

Fig. 32. Microstructure of transient network of micelles in presence of Naphthols.

References

1. Candau, S.J & Lequeux, F., *Current Opinion In Colloid and Interface* Science, **2**, 420 (1997).
2. Evans, D. F., and Wennerström, H., *The Colloidal Domain where Physics, Chemistry and Biology* Meet, Ed. Wiley-(1999).
3. Tanford, C. The Hydrophobic Effect, 2nd ed.; Wiley: New York,(1980).
4. Rehage, H., Hoffmann, H., *Mol. Phys.*, **74**, 933 (1991)
5. Cates, M. E., Candau, S. J., *J. Phys. Condens. Matter*, **2**, 6869 (1990).
6. Hoffmann, H., Munkert U.; Thunig, C.; Valiente, M., *J. Colloid Interface Sci.*, **163**, 217 (1994).
7. Shikata, T., Hirata, H.; Kotaka, T., *Langmuir*, **5**, 398. (1989).
8. Shikata, T., Hirata, H., Kotaka, T., *Langmuir*, **4**, 354 (1988).
9. Kern, F., Zana, R., Candau, S. J., *Langmuir*, **7**, 1344 (1991).
10. Kern, F., Lemarechal, P., Candau, S. J., Cates, M. E., *Langmuir*, **8**, 437 (1992).
11. Tornblom, M., Henriksson U., Ginley M., *J. Phys. Chem.*, 98, 7041 (1994).
12. Wang, S. Q., *J. Phys. Chem.*, 94, 8381 (1990).
13. Candau, S. J.; Hirsch, E.; Zana, R.; Adam, M., *J. Colloid Interface Sci.*, **122**, 430 (1988).
14. Hoffmann, H., Rauscher, A., Gradzielski, M., Schulz S. F., *Langmuir*, **8**, 2140 (1992).
15. Shikata, T., Morishima, Y., *Langmuir*, **12**, 5307 (1996).
16. Shikata, T., Imai, S., Morishima, Y., *Langmuir*, **13**, 5229 (1997).

17. Soltero, J. F. A., Puig, J. E., Manero, O.; Schulz, P. C., *Langmuir*, **11**, 3337 (1995).

18. Soltero, J. F. A., Puig, J. E., Manero, O., *Langmuir*, **12**, 2654 (1996).

19. Soltero, J. F. A., Bautista, F., Puig, J. E., Manero, O., *Langmuir*, **15**, 1604 (1999).

20. Hassan, P. A., Valaulikar, B. S., Manohar, C., Kern, F., Bourdieu, L., Candau, S. J., *Langmuir*, **12**, 4350 (1996).

21. Hassan, P. A., Manohar, C. J., *Phys. Chem. B*, **102**, 7120 (1998).

22. Wolff, T., Emming, C. S., von Bunau, G., Zierold, K., *Colloid Polym. Sci.*, **270**, 822 (1992).

23. Danino, D., Talmon, Y., Levy, H., Beinert, G., Zana, R., *Science*, **269**, 1420 (1995).

24. Israelachvili, J., *Intermolecular & Surface forces*, London: Academic Press (1992).

25. Majid, L. J., *J. Phys. Chem. B*, **102**, 4064 (1998) .

26. Cates, M. E., and Candau, S.J., *J. Phys : Condens. Matter*, **2**, 6869 (1990).

27. Hu, Y., Rajaram, C. V., Wang, and Jamieson, A. M., *Langmuir*, **10**, 80 (1994).

28. Hassan, P. A., Narayanan, J., Manohar, C., *Current Science*, **80**, 8 (2001).

29. Salkar, Hassan, R. A., *J. Chem. Soc., Chem. Comm.*, 1223 (1996).

30. Manohar, C., Rao, U. R., *J. Chem. Soc., Chem. Comm*, 379 (1986).

31. Turner, M. S., and Cates, M. E., *J. Phys: Condens. Matter*, **4**, 3419 (1992).

32. Cates, M. E., Candau, S. J., *J. Phys: Condens. Matter*, **2**, 6869 (1990).

33. Wunderlich, I., Rehage, H., Hoffmann, H., *Prog, Colloid Polimer Science*, **72**, 51 (1986).

34. Odijk, T., *J. Phys. Chem.*, **93,** 3888 (1989).

35. Lindman, B.; Wennerström, H., *Top. Curr. Chem.*, **87,** 1 (1980).

36. (a) Gravsholt, S. J., *Colloid Interface Sci.*, **57,** 575 (1976).

(b) Imae, T., Kamiya, R., Ikeda, S., *J. Colloid Interface Sci.* **108,** 215 (1985).

37. (a) Gamboa, C., Sepu´lveda, S. J., *J. Colloid Interface Sci.* **1986,113,** 566.

(b) Gamboa, C.; Rý´os, H.; Sepu´lveda, S. J., *J. Chem. Phys.*, **93,** 5540 (1989).

38. Hyde, A. J.; Johnstone, D. W. M., *J. Colloid Interface Sci.,* **53,** 349 (1975).

39. (a) Yatcilla, M. T., Herrington, K. L., Brasher, L. L., Kaler, E. W., Chiruvolu, S., Zasadzinski, J. A., *J. Phys. Chem.*, **100,** 5874 (1996).

(b) So¨derman, O., Herrington, K. L., Kaler, E. W., Miller, D. D., *Langmuir*, **13,** 5531 (1997).

40. Cates, M. E., Candau, S. J., J. *Phys. Condens. Matter*, **2,** 6869 (1990).

41. Rehage, H., Hoffmann, H., *Mol. Phys.*, **74,** 933 (1991).

42. Rao, U. R. K., Manohar, C., Valaulikar, B. S., Iyer, R. M., *J. Phys. Chem.*, **91,** 3286 (1987).

43. Bijma, K., Rank, E., Engberts, J. B. F. N., *J. Colloid Interface Sci.*, **205,** 245 (1998).

44. Olsson, U., So¨derman, O., Gue´ring, P., *J. Phys. Chem.*, **90,** 5223 (1986).

45. Manohar, C., Rao, U. R. K., Valaulikar, B. S., Iyer, R. M., *J. Chem. Soc.*, 379 (1996).

46. Turner, M. S., Marques, C., Cates, M. E., *Langmuir*, **6,** 695 (1993)

47. (a) Shikata, T., Sakaiguchi, Y., Urakami, H., Tamura, A., Hirata, H. J., *Colloid Interface Sci.*, **119**, 291 (1987).

(b) Sakaiguchi, Y., Shikata,T., Urakami, H., Tamura, A., Hirata, H. J., *Electron Microsc.*, **36**, 168 (1987).

(c) Sakaiguchi, Y., Shikata, T., Urakami, H., Tamura, A., Hirata, H., *Colloid Polym. Sci.*, **265,** 750 (1987).

48. (a) Lin, Z., Scriven, L. E., Davis, H. T., *Langmuir*, **8**, 2200 (1992).

(b) Clausen, T. M., Vinson, P. K., Minter, J. R., Davis, H. T., Talmon,Y., Miller, W. G., *J. Phys. Chem.*, 96, 474(1992).

49. (a) Shikata, T., Hirata, H., Kotaka, T., *Langmuir*, **3**, 1081 (1987).

(b) Imae, T., *Colloid Polym. Sci*, **267**, 707 (1989).

50. Lin, Z., Chai, J. J., Scriven, L. E., Davis, H. T., *J. Phys. Chem.*, **98**, 5984 (1994).

51. Mishra, B. K., Samant, S. D., Pradhan, P., Mishra, S. B., Manohar, C., *Langmuir*, **9**, 894 (1993).

52. Hassan, P. A., Narajanan, J., Menon, S.V.G., Salkar, R. A., Samant, S. D., Manohar, C., *Colloids Surf.*, 117, 89 (1996).

53. Berr, S. S., Caponetti, E., Johnson Jr., J. S., Jones, R. R. M., Magid, L. D., *J. Phys. Chem.*, **90**, 5766 (1986).

54. Salkar, R.A., Hassan, P.A., Samant, S.D., Valaulikar, B. S., Kumar, V. V., Kern, F., Candau, S. J., Manohar, C., *J. Chem. Soc. Chem. Commun.*, 1223 (1996).

55. Horbaschek, K., Hoffmann, H., Thunig, C., *J. Colloid Interface Sci.*, **206**, 439 (1998).

56. Menon, S. V. G., Manohar, C., Lequeux, F., *Chem. Phys. Lett.*, **263**, 727 (1996).

57. (a) Mendes, E., Narajanan, J., Oda, R., Kern, F., Candau, S. J., Manohar, S. J., *J. Phys. Chem. B*, **101**, 2256 (1997).

(b) Mendes, E., Manohar, C., Narajanan, J., *J. Phys. Chem. B*, **102**, 338 (1998).

58. Hassan, P. A., Valaulikar, B. S., Manohar, C., Kern, F., Bourdieu, L., Candau, S. J., *Langmuir*, **12**, 4350 (1996).

59. Hoffmann, H., *Viscoelastic Surfactant Solutions. In Structure and Flow in Surfactant Solutions*; Herb, C. A., Prud'homme, R. K., Eds.; *American Chemical Society*: Washington, DC, 2 (1994).

60. Yang, J., *Curr. Opin. Colloid Interface Sci.*, **7**, 276 (2002).

61. Cates, M. E., Candau, S. J., *J. Phys. Condens. Matter*, **2**, 6869 (1990).

62. Raghavan, S. R., Kaler, E. W., *Langmuir*, **17**, 300 (2001).

63. Makhloufi, R., Cressely, R., *Colloid Polym. Sci.*, **270,** 1035 (1992).

64. Ponton, A., Schott, C., Quemada, D., *Colloids Surf. A*, **145**, 37, (1998).

65. Rehage, H. and Hoffmann, H., *Mol. Phys.*, **74**, 933 (1991).

66. Bhattacharya, S. and De, S., *J. Chem. Soc., Chem. Comm.*, 651 (1995).

67. Bhattacharya, S. and De, S., *Langmuir*, **15**, 3400 (1999).

68. Bhattacharya, S., De, S. M. and Subramanian, M., *J. Org. Chem.*, **63**, 7640 (1998).

69. Bhattacharya, S. and De, S., *J. Chem. Soc., Chem. Commun.*, 1283 (1996).

70. Fukuda, H., Kawata, K., Okuda, H. and Regen, S. L., *J. Am.Chem. Soc.*, **112**, 1635 (1990).

71. Kobuke, Y., Ueda, K. and Sokabe, M., *J. Am. Chem. Soc.*, **114**, 7618 (1992).

72. Yatcilla, M. T., Herrington, K. L., Brasher, L. L., Kaler, E. W.,Chiruvolu, S. and Zasadzinski, J. A., *J. Phys. Chem.*, **100**, 5874 (1996).

73. Marques, E., Khan, A., de Graca Miguel, M. and Lindman, B., *J. Phys. Chem.*, **97**, 4729 (1993).

74. Brasher, L. L., Herrington, K. L. and Kaler, E. W., *Langmuir*, **11**, 4267 (1995)

75. Magid, L. J., Han, Z., Warr, G. G., Cassidy, M. A., Butler, P. D. and Hamilton, W. A., *J. Phys. Chem. B*, **101**, 7919 (1997).

76. Mishra, B. K., Samant, S. D., Pradhan, P., Sushama, B., Mishra and Manohar, C., *Langmuir*, **9**, 894 (1993).

77. Carver, M., Smith, T. L., Gee, J. C., Delichere, A., Caponetti, E. and Magid, L. J., *Langmuir*, **12**, 691 (1996).

78. Kreke, P. J., Magid, L. J. and Gee, J. C., *Langmuir*, **12**, 699 (1996).

79. Bachofer, S. J. and Simonis, U., *Langmuir*, **12**, 1744 (1996).

80. Long, M. A., Kaler, E. W. and Lee, S. P., *Biophys. J.*, **67**, 1733 (1994).

81. Zemb, T., Dubois, M., Deme, B. and Gulikkrzywicki, T., *Science*, **283**, 816 (1999).

82. Oda, R., Huc, I., Schmutz, M., Candau, S. J. and Mackintosh, F. C., *Nature*, **399**, 566 (1999).

83. Edwards, K., Gustaffson, J., Almgren, M. and Karlsson, G., *J. Colloid. Int. Sci.*, **161**, 299 (1993).

84. Friberg, S. E., Campbell, S., Fei, L, Yang, H., Patel, R. and Aikens, P. A., *Coll. Surf. A*, **129**, 167 (1997).

85. Kaler, E. W., Herrigton, K. L., Murthy, A. K. and Zasadzinski,J. A. N., *J. Phys. Chem.*, **96**, 6698 (1992).

86. Cohen, D. E., Thurston, G. M., Chamberlin, R. A., Benedek, G. B. and Carey, M. C., *Biochemistry*, **37**, 14798 (1998).

87. Pedersen, J. S., Egelhaaf, S. U. and Schurtenberger, P., *J. Phys. Chem.*, **99**, 1299 (1995).

88. de la Maza, A. and Parra, J. L., *Langmuir*, **11**, 2435 (1995).

89. Egelhaaf, S. U. and Schurtenberger, P., *Phys. Rev. Lett.*, **82**, 2804 (1999).

90. Egelhaaf, S. U. and, Schurtenberger, P., *Phys. B*, **234**, 276 (1997).

91. Oda, R., Bourdieu, L. and Schmutz, M., *J. Phys. Chem. B*, **101**, 5913 (1997).

92. Inoue, T., Motoyama, R., Miyakawa, K. and Shimozawa, R., *J. Colloid Interface Sci.*, **156**, 311 (1993).

93. Cariontaravella, B., Chopineau, J., Ollivon, M., Lesieur, S., *Langmuir*, **14**, 3767 (1998).

94. Forte, L., Andrieux, K., Keller, G., Grabiellemadelmont, C., Lesieur, S., Paternostre, M., Ollivon, M., Bourgaux, C. and Lesieur, P., *J. Thermal Analysis Calorimetry*, **51**, 773 (1998).

95. Dubachev, G. E., Polozova, A. I., Simonova, T. N., Borovyagin, V. L., Demin, V. V. and Barsukov, L. I., *Biol. Membr.*, **13**, 100 (1996).

96. Keller, S. L., Bottenhagen, P., Pine, D. J., Zasadzinski, J. A., *Phys. Rev. Letters*, **80**, 2725 (1998).

97. Kalur, G. C., Frounfelker, B. D., Cipriano, B. H., Norman, A. I., Raghavan, S. R., *Langmuir*, **21**, 10998 (2005).

98. Rao, U. R. K., Manohar, C., Valaulikar, B. S., Iyer, R. M., *J. Phys. Chem.*, **91**, 3286 (1987).